Post Access Report

Numerical simulation and analysis of the MADWEC wave energy converter

Awardee: University of Massachusetts Dartmouth

Awardee point of contact: Dr. Mehdi Raessi

Facility: WEC-Sim (Wave Energy Converter SIMulator) – Numerical Modeling, Design, and Data Analysis

Facility point of contact: Dr. Nathan Tom

Date: October 27, 2023

TEAMER
Testing & Expertise for Marine Energy

EXECUTIVE SUMMARY

The wave energy converter (WEC) developed at the University of Massachusetts Dartmouth is called MADWEC, which stands for maximal asymmetric drag WEC. MADWEC is a point absorber device and designed to be low-cost, low-maintenance, and easily deployable. The main MADWEC components are the buoy, power take-off (PTO), and tethered ballast system. A major cost-saving has been achieved through the tethered ballast system (US Patent 11,156,200 B2), which is a lightweight alternative to heavy and costly steel spars commonly used in point absorber WECs. The tethered ballast system is a series of nested hollow cylinders. At the bottom of each hollow cylinder, there are louvres that open as the ballast system moves in a downward direction, allowing the device to quickly drop in water and position itself properly relative to the free-surface waves. On the ascending half-cycle of the wave period, when the ballast system is forced to move in the upward direction, the louvres close, trapping water in the hollow cylinders and creating significant added mass that keeps the PTO relatively stationary while the buoy continues to ascend. As a result, a relative motion between the buoy and PTO is developed, which is captured by the PTO. This TEAMER support had two major objectives: 1) Optimization of the tethered ballast system design to maximize the total added mass; and 2) Building a WEC-Sim model of the MADWEC prototype and analyzing the tethered ballast and PTO performance under linear waves. Using the boundary-element method (BEM) and WAMIT software, the optimal distance between the nesting cylinders were determined to achieve the highest total added mass. The results were then used in a WEC-Sim model developed to evaluate the performance of MADWEC under various wave conditions. The WEC-Sim model also includes Simulink models of the PTO that follow the bench-top prototype model of UMassD. The preliminary WEC-Sim results suggest that the total added mass of the ballast system, which plays a key role in the system dynamics, can be increased to enhance the performance. The WEC-Sim analysis also helped capture the natural frequency and resonance phenomenon found in the multibody WEC system.

1 INTRODUCTION TO THE PROJECT

This project provides technical assistance to the development of a wave energy converter (WEC) device developed at the University of Massachusetts Dartmouth (UMassD). The device is called MADWEC, which stands for maximal asymmetric drag wave energy converter. It is a point absorber device designed to be low-cost, low-maintenance, and easily deployable. Guided by cost-saving initiatives, MADWEC uses several "off-the-shelf" parts, including a regular garage door spring, commercially available one-way clutch and electric generators, etc. Through computational simulations, this TEAMER project will help optimize the tethered ballast system, investigate the performance of MADWEC under linear waves, and estimate its power output. Specifically, technical assistance will be provided for the following two tasks:

Task 1: Optimization of the tethered ballast system design to maximize the total added mass.

Task 2: Building a WEC-Sim model of the MADWEC prototype and analyzing the tethered ballast and PTO performance under linear waves.

Task 1 is focused on determining the optimal spacing between a series of nested hollow cylinders as their radii progressively decrease in order to maximize the total added mass of the series. To further illustrate, suppose the added mass of a single hollow cylinder is m_a. The total added of mass of two identical cylinders spaced at a very large distance, L, is expected to be $2m_a$ because there is no interaction between the cylinders. As the spacing decreases, the interaction increases, and the total added mass of the pair is expected to change. UMassD and the WEC-Sim team are seeking an optimized spacing where the total added mass of the pair is greater than $2m_a$ and is maximized. WAMIT (and/or Capytaine) BEM software will be used, and the study will be broken into five geometrical configurations each informing the next one. Configuration 1 is a single hollow cylinder placed at a water depth representative of deployment. Keeping the volume constant, the cylinder diameter, D, and cylinder height, H, will be varied to find the optimal aspect ratio, H/D, that maximizes m_a for a single hollow cylinder. Configuration 2 includes two identical hollow cylinders of given D and H (determined by Configuration 1 study) and spaced by distance L. The investigation will show at what L the total added mass of the pair is maximized, and how L depends on D and H. Configuration 3 consists of three identical hollow cylinders of a representative D and H, which are chosen from Configuration 2 and held fixed. Only the spacings between the cylinders are varied here to maximize the total added mass. Note that at the optimal point, the spacing between the 1st and 2nd cylinders, denoted by L_{12}, may be different than the spacing between the 2nd and 3rd cylinders, L_{23}. Configuration 4 investigates three nested hollow cylinders, where the largest D and H are the same as those in Configuration 3. The nesting cylinder diameter is reduced by 10% from the previous cylinder diameter. Again, only the spacings L_{12} and L_{23} are varied to maximize the total added mass. Finally, Configuration 5 includes n nested hollow cylinders ($n > 3$) and the investigation will reveal at what n (or cylinder size) the increase in the total added mass becomes negligible.

The key parameter quantified in Task 1 is the optimized cylinder spacing that maximizes the total added mass of the tethered ballast system. The total added mass of a series of nested hollow cylinders will be

quantified as a function of cylinder spacing. The optimized cylinder spacing, investigated through this support, is an important parameter that has not been explored and determined before in the tethered ballast system design.

For Task 2, WEC-Sim will be used to model the MADWEC consisting of all solid body components, including the ballast, PTO, buoy, etc., will be developed. The PTO may be one of the following: spring/mass damper system, and/or a derived transfer function of PTO between commanded and realized force/torque profile. The WEC-Sim model will be run through the following sea states: (i) Calm water (no waves) to test hydrostatic stability, (ii) Free decay (no waves) to check linear stability, verifying that radiation and hydrostatic forces are working as expected, and (iii) Regular wave runs with either (a) fixed wave heights with a vector of wave periods or (b) a constant slope (wave height is dependent on period). If time and budget allow, the MADWEC WEC-Sim model will be used to obtain preliminary results to begin populating a power matrix, which can be used for future MADWEC design and optimization efforts.

The parameters measured in Task 2 include the linear stability of the device as well as its response (amplitude and period of oscillations) to linear waves of various period and height. Additionally, the power output of the device will be measured to guide design changes to the MADWEC to improve performance. This will be the first extensive numerical simulation of the entire MADWEC system assessing its performance.

The above investigations will validate various aspects of the MADWEC design and identify areas where the performance can be improved. In addition, we plan to publish the investigation results in relevant scientific journals. Finally, from the insights gained through the above numerical simulations and the ensuing design enhancements the proposed work is expected to move the MADWEC project towards TRL 6 and needs to be matched with prototype testing

2 Roles and Responsibilities of Project Participants

2.1 Applicant Responsibilities and Tasks Performed

UMassD Team Member	Responsibility
Dr. Mehdi Raessi	UMassD manager and point of contact, distribution of mechanical PTO design and performance data from table-top model experiments, and providing details of entire MADWEC system.
Dr. Daniel MacDonald	MADWEC lead PI, distribution of technical data for MADWEC tethered ballast system for hydrodynamic modeling, and providing details of entire MADWEC system.

2.2 NETWORK FACILITY RESPONSIBILITIES AND TASKS PERFORMED

NREL Team Member(s)	Responsibility
Nathan Tom	WEC-Sim Facility Lead, management of project, oversee the ballast system added mass optimization, oversee the WEC-Sim numerical model development.
Elena Baca	WEC-Sim numerical model development and ballast system added mass optimization.
SNL Team Member(s)	**Responsibility**
Adam Keester	WEC-Sim numerical model development and ballast system added mass optimization.

3 PROJECT OBJECTIVES

TASK 1: Provide WAMIT (and/or Capytaine) support to maximize the total added mass in heave for three hollow cylinders.

- **Subtask 1:** Single cylinder placed at a water depth representative of deployment. Select a desired volume and then iterate across various cylinder diameter, D, and height, H, combinations to maintain same desired volume (where desired volume would be the solid volume of a cylinder with the same geometric parameters). This will help identify if squat cylinders verse elongated cylinders generate large added mass values. This information will help with initial selection in Subtasks 2 – 5.
  - **Output metric**: Maximize heave added mass and report optimum dimensions.
- **Subtask 2**: Two identical hollow cylinders of diameter, D, and height, H, are spaced apart by separation distance, L_s. The investigation will determine at what L_s the total heave added mass is maximized.
  - **Optimization parameters:** Spacing, L_s , between two hollow cylinders will be varied, cylinder diameter, D, and cylinder height, H.
  - **Output metric:** Maximize the heave added mass that is normalized by twice the heave added mass of an isolated hollow cylinders of diameter, D, and height, H.
- **Subtask 3:** Three identical hollow cylinders of a representative D and H, are chosen from Subtask 2 and held fixed. Only spacing L_{12} and L_{23} are varied to maximize the total heave added mass relative to the displaced fluid mass of the cylinders assuming they were prismatic solid cylinders. The WEC-Sim Facility team should be able to compare this study to Subtask 2 to see if there is any interaction between multiple cylinders that might enhance the total added mass, or can they be thought of simply as a series of independent hollow cylinders:
  - **Optimization parameters**: Spacing between adjacent hollow cylinders, L_{12} and L_{23}, will be varied where the separation distance is normalized by a single hollow cylinder height.
  - **Output metric**: Maximize the heave added mass contributions across all three hollow cylinders that are normalized by three times the added mass of single isolated hollow cylinder.

  - ***Notes***: If the cylinders are placed sufficiently below the free surface, the cylinders could be assumed to be oscillating in an infinite fluid and the team can use analytical formulas as a benchmark.
- **Subtask 4**: Three nested hollow cylinders, where the largest diameter and height are equal to those of selected in Subtask 3:
  - **Optimization parameters**: Spacing between adjacent hollow cylinders adjacent hollow cylinders, L_{12} and L_{23}, will be varied where the separation distance is normalized by a single hollow cylinder height. Furthermore, the diameter of the nested cylinders to be reduced by 5-10% per UMassD discretion after reviewing results from Subtasks 1-3.
  - **Output metric**: Maximize the heave added mass contributions that are normalized by the added mass of isolated hollow cylinders that make up the nesting configuration.
- **Subtask 5**: Adding to Subtask 4, there are now n nested hollow cylinders (n > 3). The award team would like to know at what n the increase in heave added mass becomes negligible.
  - **Optimization parameters**: Spacing between adjacent hollow cylinders, L_s, will be set constant for this exploration or else the number of design variables makes the problem intractable. The number of nested cylinders, n, where additional nested cylinders can be added until the growth in heave added mass is negligible (i.e. no additional positive interaction.

NREL/SNL shall complete the following:

- NREL/SNL WEC-Sim team will be responsible for developing the CAD models, associated meshes, and running the appropriate BEM solver to generate the hydrodynamic radiation coefficients that will be used to evaluate the performance of the tethered ballast system.

UMassD shall complete the following:

- UMassD will provide the SNL/NREL team with the upper and lower limits on the hollow cylinder diameter and height as well as the maximum separation distance between the first and last hollow cylinder to limit the optimization search space. Furthermore, UMassD will be responsible for reviewing analysis results after each Subtask completion in order to make decisions on hollow cylinder sizes that will be used in the subsequent Subtasks.

TASK 2: Development of a WEC-Sim model of the MADWEC Concept.

- **Subtask 1:** Use available CAD, or solid body models, of each MADWEC component to mesh for import to WAMIT (and or Capytaine) to generate the hydrodynamic coefficients.
  - If these components are already available from UMD this subtask could have a reduced number of hours; however, past experience has shown that edits (often defeaturing) to CAD models are generally still required to generate a mesh of the outer WEC hull that will be accepted and provide usable inputs into WEC-Sim.
- **Subtask 2:** Build the WEC-Sim model to include all solid bodies, simple spring-damper power-take-off design, and mooring. If other auxiliary systems desired by UMassD for inclusion in the WEC-Sim model that will require more time and funds to incorporate, UMassD and the WEC-Sim Facility will discuss what work scope could be descoped in other subtasks to stay on time and budget.
- **Subtask 3**: In Subtask 2 a simple PTO model will be used for initial development of the WEC-Sim model. UMD has confirmed the desire to update to a higher fidelity model that is more representative of their PTO design. The potential PTOs discussed to date are described in the

following bullets, but only one option will be pursued in this award and the decision will be made between UMassD and the WEC-Sim Facility.
  - Experimentally derived transfer function of PTO between commanded and realized force/torque profile
- **Subtask 4:** The WEC-Sim model will be run through the following sea states for verification:
  - Calm water (no waves) to test hydrostatic stability,
  - Free decay (no waves) to check linear stability of model when displaced from equilibrium,
    - Verify radiation and hydrostatic forces are working as expected.
  - Regular wave runs
    - 2-3 wave heights with a vector of wave periods or a constant slope where the wave height is adjusted based on the wave period.
  - Power matrix
    - This task will be dependent on project progress and left as a final task if time and funds are available. If time and funds are not available, UMassD will be instructed on how to use the verified WEC-Sim model to develop their own power matrix.

NREL/SNL shall complete the following:

- NREL/SNL WEC-Sim team will be responsible for developing the CAD models, associated meshes, and running the appropriate BEM solver to generate the hydrodynamic radiation coefficients for each physical component (with hydrodynamic relevance) that will be used in the WEC-Sim model. In addition, the WEC-Sim team will build the WEC-Sim model which incorporates a simplified PTO model and one higher fidelity PTO model as described in Subtask 3. The NREL/SNL WEC-Sim team will then simulate the WEC-Sim model in a variety of wave conditions to check the accuracy and functionality of the model prior to handing all project files to UMassD.

UMassD shall complete the following:

- UMassD will work with the SNL/NREL team to provide their desired PTO properties, PTO models, and test data to assist in coupling a higher fidelity PTO model within WEC-Sim. Based on the PTO information presented to the WEC-Sim Team, the WEC-Sim Team may ask for further details or additional post processing of UMassD's experimental data in order to get it in a form that the WEC-Sim Team can readily use. UMassD will also be responsible for providing any CAD models of existing hull structures, mass properties of each solid body (see Figure 1), and other information necessary to develop a dynamic model (such as target buoyancy values).

TASK 3: Data analytics and post processing

NREL/SNL shall complete the following:

- For each subtask in Task 1, the WEC-Sim team will report the following:
  - Maximum heave added mass values and the corresponding geometry and separation distances.
  - If possible, the WEC-Sim team will attempt to generate surface or contour plots that illustrate how the total heave added mass changes based on the optimization parameters.
- For Subtask 4 in Task 2, the WEC-Sim team will report the following
  - Peak, average, and RMS results will be calculated for:
    - PTO mechanical power, velocity, and force,

- PTO electrical power
- Heave displacements for each hydrodynamic body in the WEC-Sim model

UMassD shall complete the following:

- UMassD will approve the sea conditions (i.e. wave height and period) that WEC-Sim will be simulated in to calculate the desired performance metrics. The initial set of sea conditions will need to be provided to the SNL/NREL WEC-Sim team prior to the start of this task. NREL and SNL will need to approve the list of sea conditions ensure there is sufficient time and funding to complete the simulation test matrix.

TASK 4: Reporting and Technology Transfer

NREL/SNL shall complete the following:

Provide the following to DOE Office of Scientific and Technical Information (OSTI):

- An initial abstract suitable for public release at the time of the CRADA is executed.
- A final report, within thirty (30) days upon completion or termination of this CRADA, to include a list of Subject Inventions.
- Other scientific and technical information in any format or medium that is produced as a restore of this CRADA.

Provide the following to TEAMER:

- Post Access Report within sixty (60) days upon completion of the award.

UMassD shall complete the following:

UMassD will provide feedback to the SNL/NREL team on the final close out documentation as listed in the NREL Task 4 above. UMassD will be given at least two weeks to review the final documents that NREL and SNL will write to close out the project. UMassD will need to submit any requests for changes to the reports no later than 1 week before the end of the agreement or an earlier submission date agreed upon by all parties.

4 Test Facility, Equipment, Software, and Technical Expertise

NREL and SNL develops, validates, and disseminates the open-source Wave Energy Converter SIMulator (WEC-Sim). The code is developed in MATLAB/SIMULINK using the multi-body dynamics solver Simscape Multibody. WEC-Sim has the ability to model devices composed of rigid bodies, joints, power take-off systems, and mooring systems. Simulations are performed in the time-domain by solving the governing wave energy converter equations of motion in six degrees of freedom. The model can be used to simulate WEC device dynamics and performance in operational and extreme waves, allowing for improvement of WEC performance during the design process. The WEC-Sim Facility team has the technical expertise, extensive experience, and the tools required to perform numerical simulations of wave energy converters. The WEC-Sim Facility team has many years of experience using hydrodynamic BEM codes (i.e. WAMIT, NEMOH, Capytaine, etc.) and WEC-Sim software packages that will be used for the proposed work.

A member of the NREL team, Dr. Nathan Tom, has served as a Co-PI on various (unfunded) grant proposals previously submitted by UMass-Dartmouth to advance the MADWEC design. As a result, he is fairly familiar with the device and its envisioned applications. The scope of the TEAMER project was devised in collaboration and close communication with Dr. Nathan Tom (NREL).

5 TEST OR ANALYSIS ARTICLE DESCRIPTION

Our proposed wave energy converter (WEC) is called MADWEC, which stands for maximal asymmetric drag wave energy converter, and is shown in Figure 1 of the attachment. MADWEC is a point absorber device and designed to be low-cost, low-maintenance, and easily deployable. The main MADWEC components are the buoy, power take-off (PTO), and tethered ballast system (see Figure 1). Guided by cost-saving initiatives, we designed the PTO using "off-the-shelf" parts, which include a regular garage door spring, commercially available one-way clutch and electric generators, etc. More importantly, a major cost-saving has been achieved through the tethered ballast system (US Patent 11,156,200 B2), which is a lightweight alternative to heavy and costly steel spars commonly used in point absorber WECs. The tethered ballast system is a series of nested hollow cylinders (see Figure 1). At the bottom of each hollow cylinder, there are louvres that open as the ballast system moves in a downward direction, allowing the device to quickly drop in water and position itself properly relative to the free-surface waves, as shown in Figure 2 of the attachment. On the ascending half-cycle of the wave period, when the ballast system is forced to move in the upward direction, the louvres close, trapping water in the hollow cylinders and creating significant added mass that keeps the PTO relatively stationary while the buoy continues to ascend. As a result, a relative motion between the buoy and PTO is developed, which is captured by the PTO and converted into electrical energy stored in the battery bank. The modular PTO design allows multiple triplets of generators feeding the modular battery bank that can be used to power a range of applications, from oceanographic sensors and monitoring systems to charging AUVs.

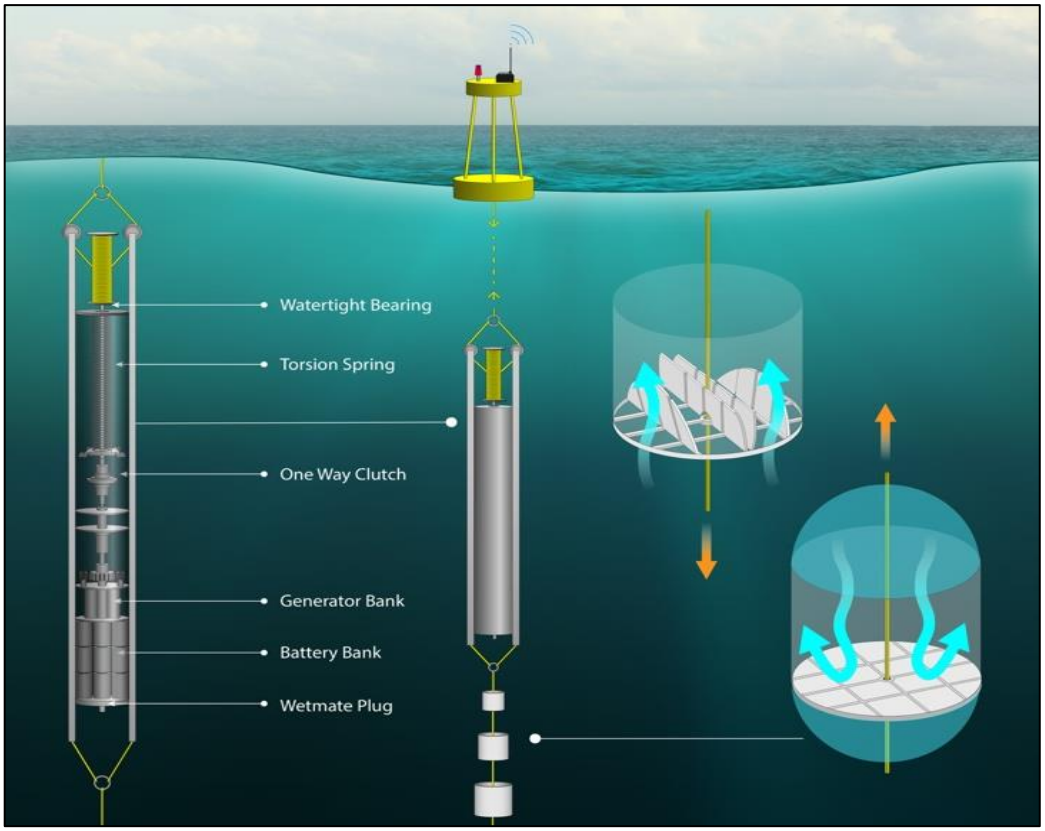

Figure 1 - Schematic rendering of MADWEC deployment (center), with action of tethered ballast component on descent (l) and ascent (r) shown to the right. Details of PTO system are shown to the left. Note that distance between the water surface and first ballast component would be approximately half of the expected dominant wavelength.

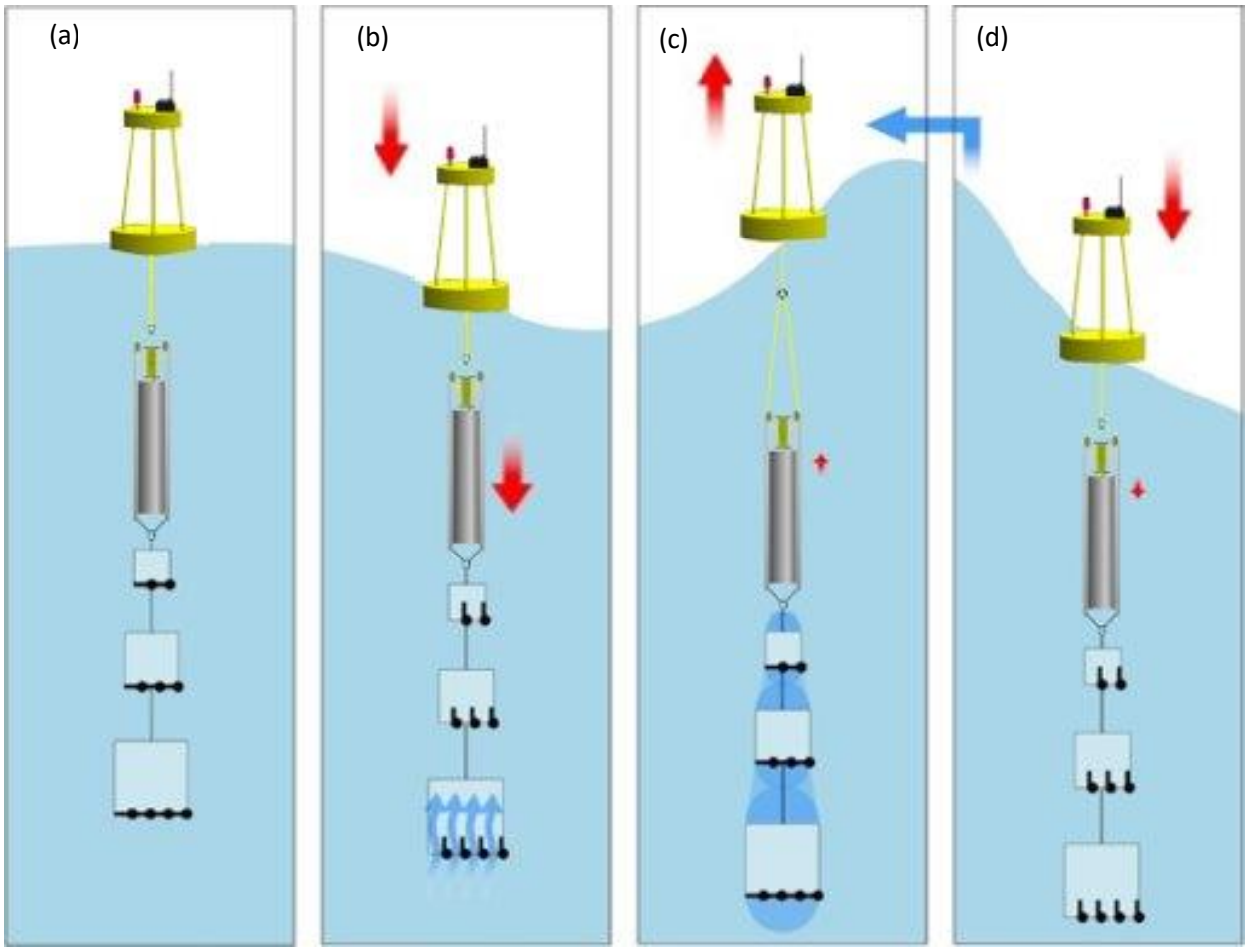

*Figure **2** - Operating principle of tethered MADWEC system. With no waves present (a), the system is at rest, with the louvers closed. As a wave trough approaches (b), the louvers open, providing minimal added mass, and the device drops quickly into the wave trough. As a wave crest approaches (c), upward motion results in closing of the louvers, yielding maximal added mass (note additional added mass trapped between ballast components), and power is generated as the buoy responds to the oncoming wave. On each successive trough (d), the system resets into the wave trough to maximize power generation.*

6 WORK PLAN

6.1 NUMERICAL MODEL DESCRIPTION

WEC-Sim is a mid-fidelity WEC numerical modelling tool based on linear potential flow theory. Hence, the wave field is considered to be a linear superposition of incident, radiated and diffracted regular wave components. Boundary Element Method (BEM) codes are used to compute a body's hydrodynamic coefficients (e.g. added mass, damping, excitation force) for a range of discrete frequencies. BEMIO is then used to pre-process the hydrodynamic coefficients and save them to a .h5 file that can be read by WEC-Sim. WEC-Sim then uses these frequency-domain coefficients in time-domain formulations of the hydrodynamic forces. This conversion is required to model the WEC system in the time-domain, which is necessary to include non-linearities in the system - such as joints, PTOs, control systems, moorings etc. A complete description of the code's theory is available on the WEC-Sim website: https://wec-sim.github.io/WEC-Sim/man/theory.html The accuracy of WEC-Sim has been verified in code-to-code comparisons and validated against experimental data. A full list of relevant publications is also available on the WEC-Sim website: https://wec-sim.github.io/WEC-Sim/man/publications.html

A key input into WEC-Sim is the hydrodynamic radiation and diffraction coefficients that define the forces the WEC experiences when oscillating within the wave environment. These hydrodynamic coefficients are frequently obtained from Boundary Element Method hydrodynamic solvers which assumes the fluid structure interaction can be adequately described by linear potential flow theory. Many researchers in the offshore field will be familiar with BEM codes such as WAMIT, NEMOH, Capytaine, and AQWA which all can be used as input into WEC-Sim. WAMIT is a commercial code, developed at the Massachusetts Institute of Technology (MIT), and is considered by many to be the gold standard in the research community. NEMOH and Capytaine are both open source codes that provide a lower cost of entry for developers and researchers, but suffer from known inadequacies and do not have the same support as WAMIT (NEMOH has had no active development for several years now). The WEC-Sim team plans to develop hydrodynamic models from both WAMIT and Capytaine to provide a code-to-code comparison as well as a template for UMassD to use WAMIT or Capytaine to continue their own MADWEC development.

6.2 TEST AND ANALYSIS MATRIX AND SCHEDULE

Table 1 – Deliverables, Responsibilities and Estimated Completion Date. Project timeline and completions dates will be updated as the project progresses.

Task No.	Task Name	Duration (Months) (Start)	(Finish)	Responsible Party
0	Provide MADWEC design details, existing CAD models, and other information relevant to building a WEC-Sim model to NREL/SNL.	On execution of the Agreement		UMassD
1	Provide WAMIT (and/or Capytaine) support to maximize the total added mass in heave for three hollow	From execution of the Agreement	4 months from execution of the Agreement	SNL/NREL

	cylinders			
2	Development of a WEC-Sim model of the MADWEC Concept	5 months from execution of the Agreement	8 months from execution of the Agreement	SNL/NREL
3	Data analytics and post processing	9 months from execution of Agreement	10 months from execution of the Agreement	SNL/NREL
4	Reporting: Complete TEAMER Post Access Report	On completion of the Agreement		SNL/NREL/ UMassD

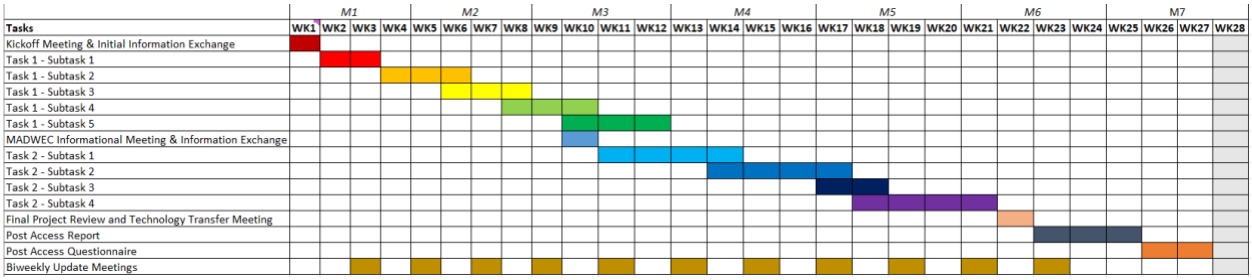

Figure 3: Project Proposed Schedule

6.3 Safety

The project will not require any in-person or physical testing and analysis will be completed as a desktop study. Applicable office safety standards will be followed.

6.4 Contingency Plans

This work in this award will be completely numerical and the only data set that UMassD would like to incorporate into the WEC-Sim model is already available. Therefore, the WEC-Sim Facility team at this time has not identified any project dependencies that could potentially delay the project or result in not delivering on the project milestones. However, the complexity of the models and analysis may exceed the WEC-Sim Facility's initial estimates which could result in de-scoping some of the work such that the award can be completed on time and on budget.

6.5 Data Management, Processing, and Analysis

6.5.1 Data Management

WEC-Sim-generated data will be stored locally on the machine the code is run on and backed up using GitHub. The final dataset containing results from the numerical modelling campaign will uploaded to MHK DR.

6.5.2 Data Processing

WEC-Sim saves the data from each run as a .mat file (binary), which can be read into memory with MATLAB or Python for post-processing. Meaningful directory and file names will be used for clarity and figures will be provided with accompanying post processing scripts attached for complete traceability and reproducibility.

6.5.3 Data Analysis

As discussed in Task 3 in Section 3, the data analysis for both tasks will be completed either using Excel or MATLAB. For Task 1, the analysis will be focused on collecting and visualizing the radiation heave added mass for the various hollow cylinder configurations. For Task 1 there is no dynamic analysis and the results will be stored as vectors or arrays with of the heave added mass coefficients against oscillation frequency, cylinder geometry, and cylinder separation. For Task 2, the WEC-Sim model allows for the dynamic simulation of the MADWEC under different sea conditions. Specifically for Subtask 4 in Task 2, the quantities of interest that will be measured and reported during regular wave simulations will include peak, average, and RMS results on the PTO performance and displacement (motion) of each hydrodynamic body in the WEC-Sim model.

7 PROJECT OUTCOMES

7.1 RESULTS

- **Task 1 Boundary Element Method Modeling**

Boundary Element Method Set-up

The geometry for Task 1 is modeled as an open-top, thin-walled cylinder. The geometry is intended to vary in WEC-Sim, with the cylinder's base opening and closing. For the purposes of maximizing the heave added mass in Task 1, only the closed-base cylinder is relevant as it has far more added mass than an open-base cylinder. Here, for convenience, "cylinder" will refer to this specific version of a cylinder with no top surface but with a closed base, see Figure 1. Also "added mass" here will always refer to added mass in the heave (vertical) direction.

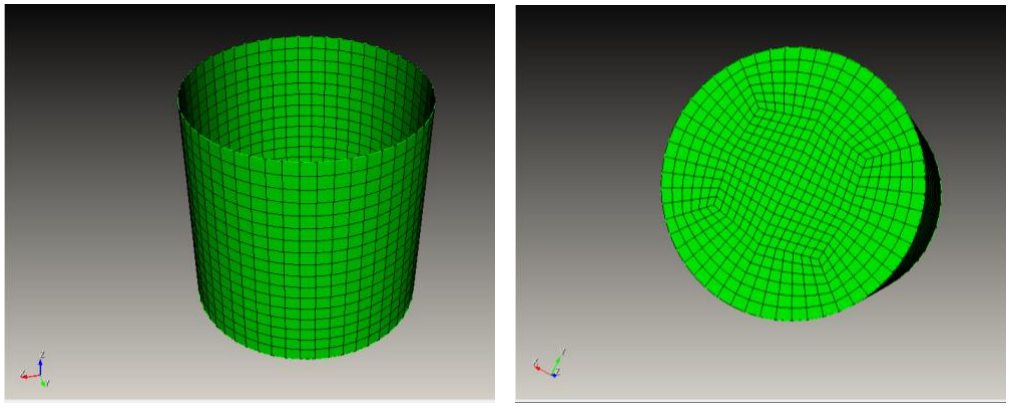

Figure 1. CUBIT visualization of the cylindrical geometry used in this study. Left, top-down view showing the open top. Right, bottom-up view showing the closed base.

There are several WAMIT methods applicable to this geometry. It is desirable to use the most accurate and least computationally expensive method available. WAMIT's conventional lower-order method requires a surface mesh to represent the geometry. It is easy to use, but more computationally expensive when simulating many cases. WAMIT's higher-order analytical method takes additional up-front set-up but can be more accurate and is faster. The higher-order method does not approximate the geometry with a surface mesh, but instead defines the surface exactly using panels. In this case, each cylinder can be represented by exactly two panels in cylindrical coordinates. When the x-plane and y-plane symmetries of the shape are considered, the two representative panels are a quarter-circular base, and a curved sheet, as shown in Figure 2.

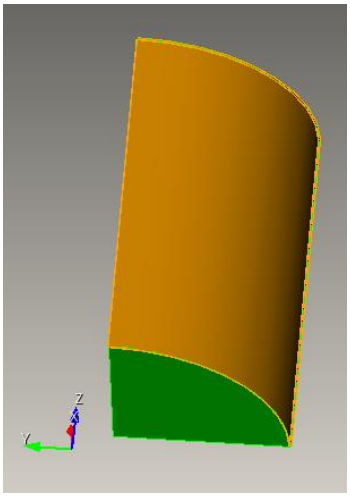

Figure 2. Higher-order analytical panels. Green, quarter-circular base. Orange, curved cylindrical shell.

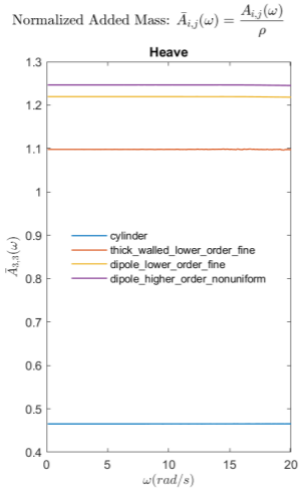

Figure 3. Comparison of the heave added mass for various relevant WAMIT methods.

Fortunately, WAMIT contains an identical, pre-built analytical shape (CIRCCYL, i.e. circular cylinder) in its packaged Fortran function (geomxact.f). This pre-built model is used for Tasks 1.1 and 1.2 to represent UMD's cylinder. Additionally, the cylinder is represented using WAMIT's dipole method, meaning the walls are infinitely thin plates. Defining the surfaces as dipoles increases the simulation speed, allows the use of the pre-built analytical geometry, and removes numerical problems that arise from defining very thin walls.

Several tests are conducted across WAMIT methods to ensure that the higher-order analytical cylinder is valid to use in this scenario. Figure 3 shows a comparison between various WAMIT methods including, in estimated order of accuracy: an enclosed cylinder, thick-walled lower-order (meshed) cylinder, dipole lower-order (meshed) cylinder, and dipole higher-order (analytical) cylinder. There is some variation in the resultant added mass, but the two most accurate methods are within 5% of each other, giving credence to this higher-order method. Additionally, Figure 3 shows that there is no discernible frequency-dependence at this depth. This greatly simplifies the presentation and interpretation of the added mass results, since a single value can accurately represent the entire frequency range.

Figure 4 shows the effect of deployment depth on the hydrodynamics. Added mass largely depends neither on frequency nor deployment depth (note the scale is very zoomed in). Heave radiation damping and excitation force magnitude do depend on depth, but do not change significantly beyond 30m. A deployment depth of 50m is chosen for Task 1.1 and the topmost cylinders of Tasks 1.2-1.3. A deployment depth of 75m is chosen for the lowest cylinder in Tasks 1.4-1.5 to ensure that the added mass is depth-independent for all cylinders, especially for these cases which contain many cylinders.

In the Task 2 WEC-Sim model, the cylinders will be considered as a single rigid body for convenience and speed. However, the given higher-order analytical method cannot place multiple cylinders into a single body. Figure 5 shows that multiple cylinders can be represented as distinct bodies in WAMIT, then combined into a single system when analyzing the added mass. The results of a 2-cylinder, 2-body system can be collapsed and accurately represent a 2-cylinder, 1-body system. This multi-body set-up in Task 1 also allows UMD to obtain accurate information about the interaction between multiple cylinders.

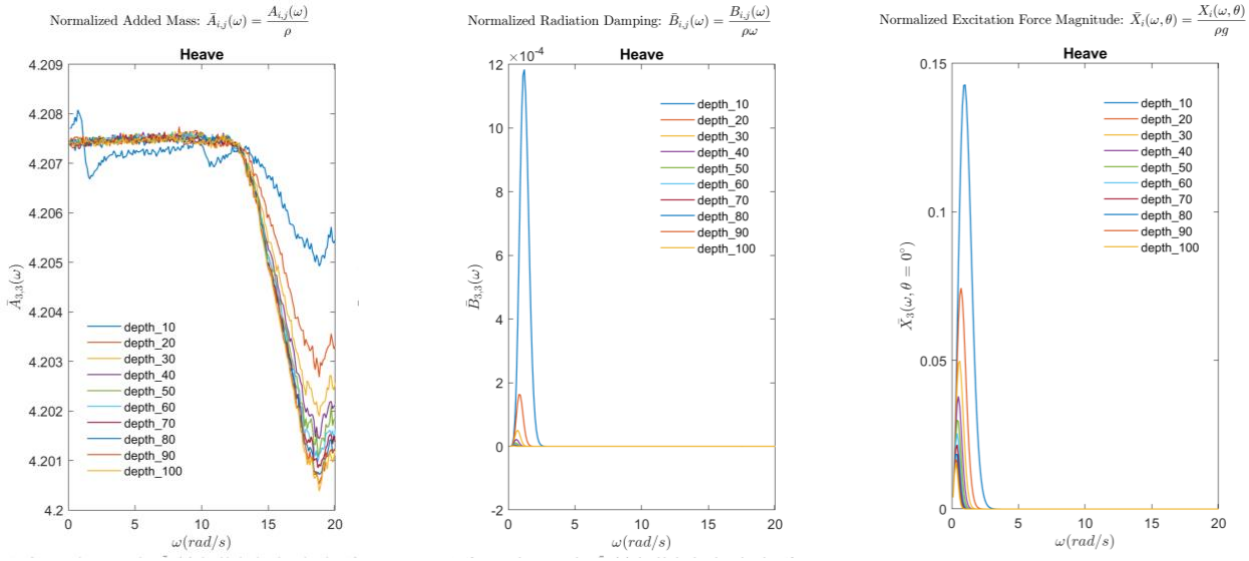

Figure 4. WAMIT results across several deployment depths.

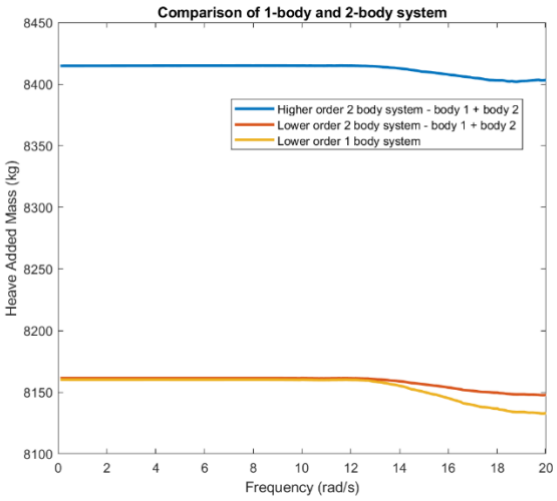

Figure 5. Interaction of bodies in multiple body and single body systems.

Given the above validation, all of Task 1 uses WAMIT's v7.2 CIRCCYL routine within the geomxact.f function to represent UMD's geometry using higher-order, analytical, open-top, dipole cylinder.

A slightly modified version of CIRCCYL was created to allow for the varied dimensions in Tasks 1.3-1.5 and is provided in the GitHub repository for reference. This custom Fortran file was compiled from an F file into a DLL file using Visual Studio 2019 (Release build, x64 platform).

Each subtask of Task 1 is created by two files, “sweepSetupSimulation.m” and “analyzeSubtaskX.m”. The first function defines the required geometry variations (sweep), writes metadata and updates WAMIT input files for each variation (setup), and calls WAMIT for each variation (simulation). The second function parses, analyzes and visualizes all relevant WAMIT results. Refer to the data repository for the scripts to recreate each part of Task 1.

- *Subtask 1.1*

The goal of Task 1.1 was to vary the dimensions of the cylinder to maximize the heave added mass. UMD provided the cylinder’s minimum and maximum height and diameter: 0.5m and 1.5 for both dimensions. The height and diameter ranges for this Subtask are listed in Table 1. Together, the ranges create 121 different cylinders that were analyzed.

Table 1. Height and diameter values in Subtask 1.1.

Heights [m]	0.5	0.6	0.7	0.8	0.9	1.0	1.1	1.2	1.3	1.4	1.5
Diameters [m]	0.5	0.6	0.7	0.8	0.9	1.0	1.1	1.2	1.3	1.4	1.5

Figures 6 and 7 show the added mass of a single cylinder across a variation in diameter and height/diameter respectively. A sphere and rectangular prism of height=diameter=1m are also shown for reference. Increasing the diameter or increasing the height result in an increase in added mass, as we expect from a larger object. The figures also show that the added mass depends more significantly on the diameter than the height. A 3x increase in diameter gives approximately a 10x increase in added mass, while a 3x increase in height only gives approximately a 2-3x increase in added mass. However, if

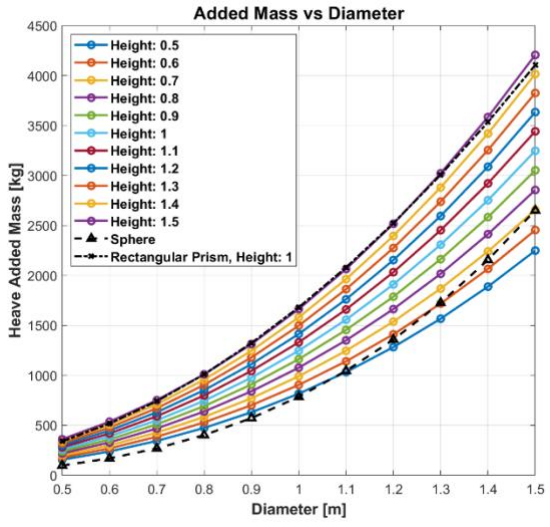

Figure 6. Added mass vs diameter

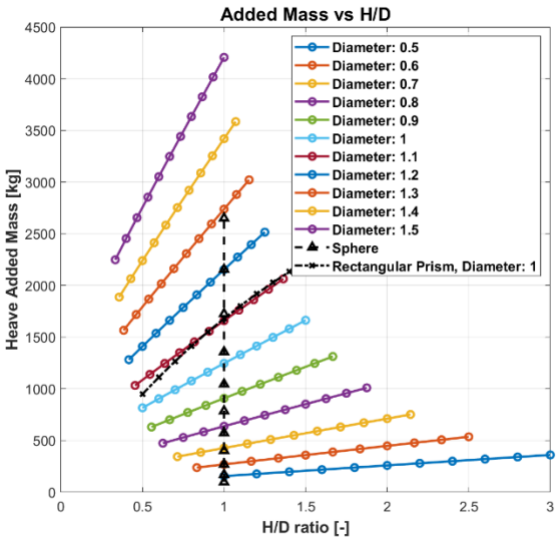

Figure 7. Added mass vs height/diameter.

any geometry within the given range of 0.5-1.5m diameter and 0.5-1.5m height is valid, then the largest dimensions should be chosen. UMD chose to continue Task 1 using the largest cylinder with a diameter and height of 1.5m.

Normalizing added mass by the displaced water mass of a shape can be informative. However, the geometries used here are made up entirely of dipoles, infinitely thin surfaces. Their displaced water mass is zero. Instead of the actual displaced water mass, we can take the water mass that the cylinder *would* enclose if it was capped and hollow as a potential surrogate. Normalizing the added mass by that displaced mass ($m_d = \rho \frac{pi}{4} D^2 h$) gives results that collapse remarkably well. Figures 8 shows the normalized added mass vs the normalized height (height/diameter). For this case of one cylinder, the

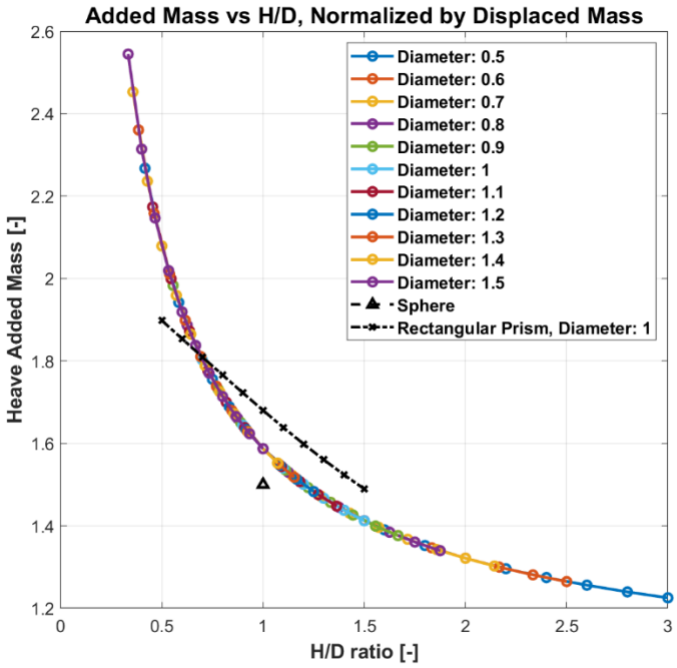

Figure 8. Normalized added mass vs the height-diameter ratio.

resulting curve fit could be used to calculate added mass and eliminate the set-up and expense inherent to a boundary element method solution.

Figure 9 shows all WAMIT results together with the corresponding power series curve fit from MATLAB's CurveFitter toolbox. The curve fit is repeated in Equation 1 for reference. The RMSE for this 121-point fit is only 2.913E-4.

$$\frac{A}{m_d} = 0.5781 * \left(\frac{H}{D}\right)^{-0.8888} + 1.009 \quad (1)$$

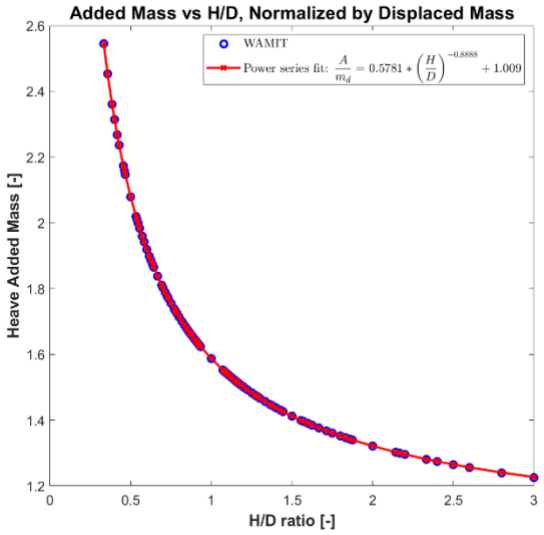

Figure 9. Normalized added mass vs normalized height. Condensed WAMIT results and the corresponding power series fit. R^2 =

- *Subtask 1.2*

Task 1.2 modeled two cylinders with a variable separation distance between them (see Figure 10). Here, the separation is considered to be the distance between the upper and lower edges of adjacent cylinders. This is not the distance between cylinder centers. The minimum separation was chosen as 0.1m while the maximum is 15m. The exact separations modeled are: 0.1, 0.25, 0.5, 0.75, 1.0, 1.5, 2.0, 2.5, 3.0, 4.0, 5.0, 7.0, 10, and 15m. Both cylinders have a height and diameter of 1.5m. The center of gravity of the topmost cylinder is at 50m depth.

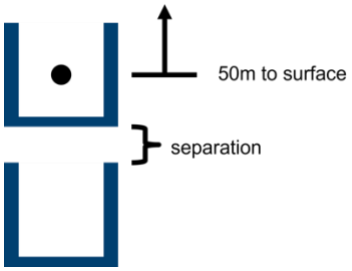

Figure 10. Illustration of the separation distance in Task 1.2.

It was predicted that, in terms of added mass, the system would act like a single cylinder of 3m height when the separation distance was extremely small and act like two independent cylinders when the separation distance was extremely large. This trend was confirmed in this task, as shown in Figure 11. At large separations (10x the diameter), the cylinders have a similar added mass to two independent cylinders. At small separations (1/10x the diameter), the cylinders trend towards the added mass of a single cylinder of double the height (3m). Figure 12 shows the net added mass of the two-cylinder system normalized by the maximum possible added mass (that of two independent cylinders, i.e. with no interactions). The boundary element method does not show any positive interaction between the cylinders, so they should be spaced far enough apart that they do not significantly interact. Considering maintenance and assembly, it's desirable to decrease the separation as much as possible while minimizing any negative interaction. The separation distance of 1.5m, equal to the diameter, is the smallest separation that still results in 95% of the possible added mass. The diameter of the system should be used as a convenient separation distance.

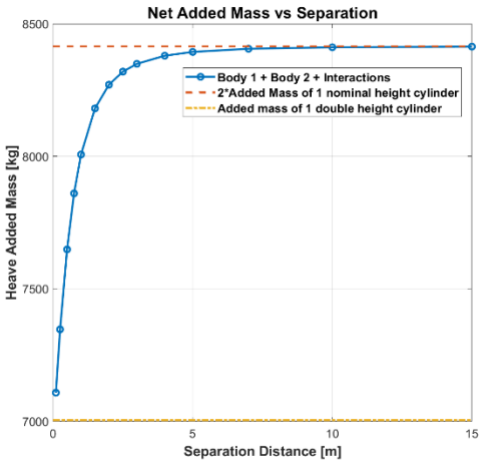

Figure 11. Net added mass of the system with the predicted values for cases of extreme separation.

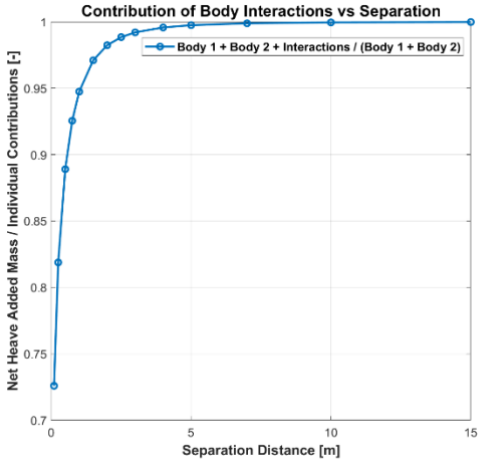

Figure 12. Net added mass of the system divided by the added mass of two independent cylinders (no negative interactions).

- *Subtask 1.3*

Task 1.3 modeled three cylinders with variable separations between each. The cylinders are fixed at the height and diameter chosen in Task 1.1 (1.5m). Both separations are varied together. As shown in Figure 13, the top-most cylinder is fixed with a center of gravity at 50m depth. The cylinders in Task 1.3 are number sequentially downwards. "S12" represents the separation between cylinders 1 and 2, "S23" represents the separation between cylinders 2 and 3.

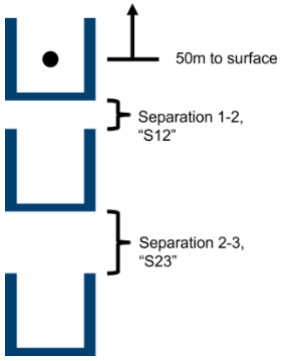

Figure 13. Illustration of the separation distances in Task 1.3.

Given the results of Task 1.2, it is assumed that the separations should not interact significantly. To save on computational expense, S12 has fewer values (0.1, 1.5, 15m) while S23 is assigned the same values as Task 1.2.

Figure 14 shows the net added mass of the three-cylinder system, with the expectations for limiting separations. As in Task 1.2, the very small separations tend to the case of cylinder that is three times the height (4.5m) while very large separations tend to the case of three independent cylinders. Figure 15 shows the system added mass normalized by the maximum possible added mass, where there is no negative interactions between cylinders.

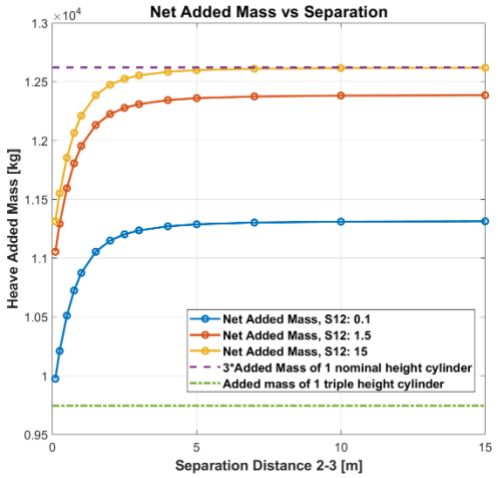

Figure 14. Net added mass vs separation distance with expectations for limiting separations.

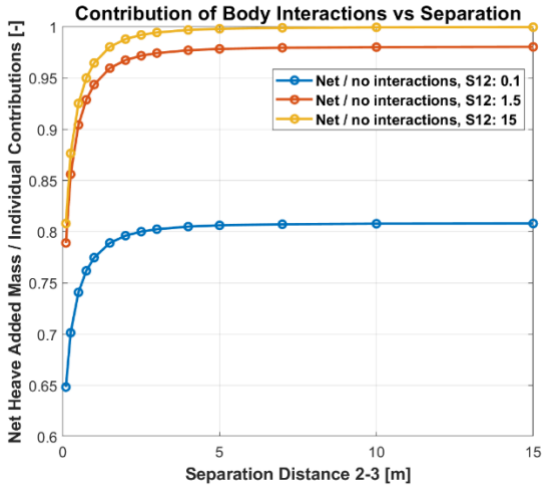

Figure 15. Normalized net added mass normalized vs separation distance.

Figure 16 shows the same information as Figures 14-15, but in a contour plot and with the separation distance normalized by the diameter. As in Task 1.2, one can get at least 95% of the possible added mass when each separation distance is equal to the diameter (1.5m).

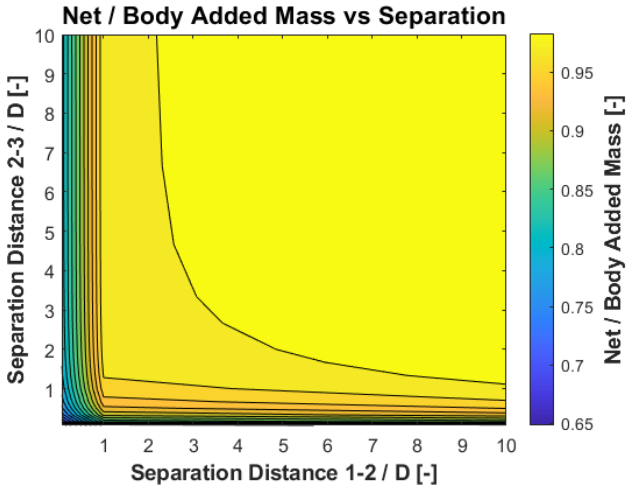

Figure 16. Normalized added mass vs normalized separation distance.

- *Subtask 1.4*

Task 1.4 is set-up similar to Task 1.3, but now the cylinders are nested and decrease in diameter as depth decreases. Three cylinders are modeled. The separation between both cylinders is varied. The largest cylinder is of diameter and height 1.5m and has its center of gravity at 75m depth. The depth was increased from Tasks 1.1-1.3 to ensure that as the number of nested cylinders increases in Task 1.5, the depth does not affect the added mass value.

The separation between cylinders 1 and 2 is "S12". The separation between cylinders 2 and 3 is "S23". Note that the lowest cylinder is now considered as #1, the middle cylinder as #2, the topmost cylinder as #3. The separations are identical to those used in Task 1.3. This numbering scheme makes it easier to represent the decrease in diameter as a function of the number of cylinders, "n". It is assumed that the diameter decreases 5% from the cylinder below it (Equation 2).

$$D_i = D_0 * 0.95^{i-1} \quad (2)$$

Figures 17 shows the normalized added mass of the system (total added mass divided by the contribution of each body, without negative interactions) vs separation distance. Figure 18 shows normalized added mass vs the separation distance normalized by the mean diameter. As in the other Task 1 subtasks, there is no positive interaction between the cylinders. The interaction between cylinders always decreases added mass. The added mass reaches 95% of its maximum value when the normalized separation distance is greater than 1.0.

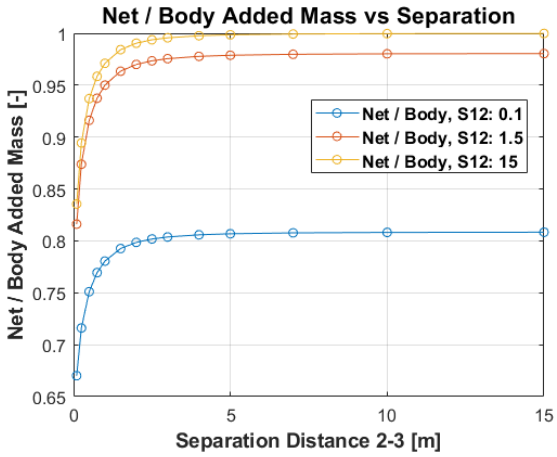

Figure 17. Normalized added mass vs separation distance.

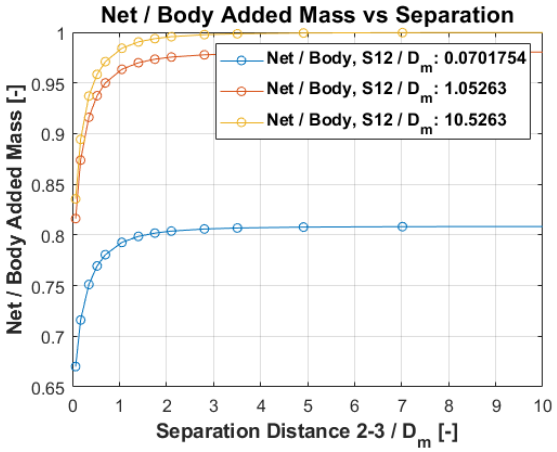

Figure 18. Normalized added mass vs separation distance normalized by the mean diameter.

- *Subtask 1.5*

Task 1.5 continued to study a series of nested cylinders. Here, the total number of cylinders varies from 2-15. The separation distance is kept constant at 1.5m. As in Task 1.4, the bottommost cylinder has its center of gravity at 75m and has a height and diameter of 1.5m.

Figure 19 shows the total added mass of the system vs the number of cylinders. Figure 20 shows the total added mass normalized by the added mass of cylinder 15. As the number of cylinders increases, the added mass always continues to increase. However, as the cylinders get smaller the additional added mass contribution decreases significantly. This aligns with the results seen in Task 1.1, where it was showed that the diameter has a much more significant effect on added mass than height.

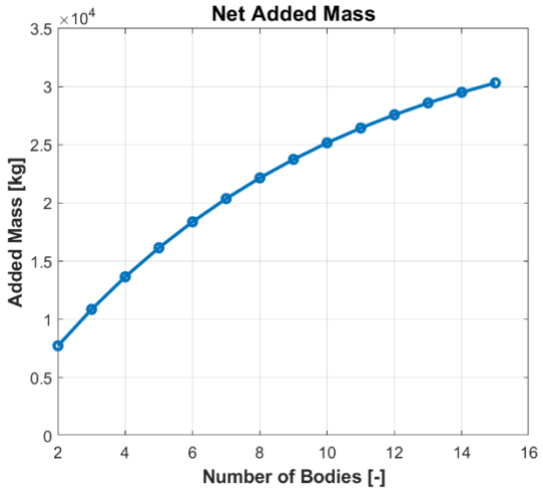

Figure 19. Net added mass vs number of cylinders.

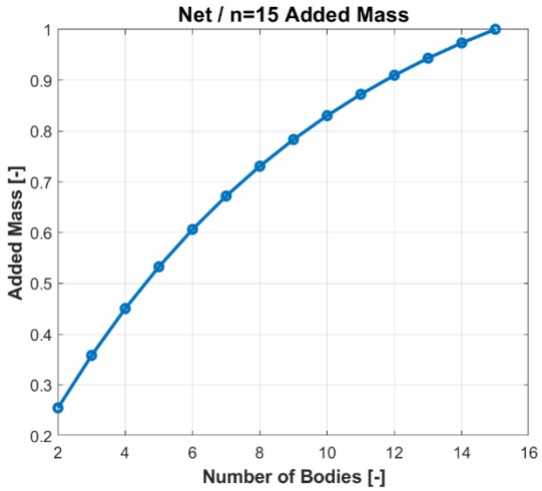

Figure 20. Normalized added mass vs number of cylinders.

Another method of visualizing the decreasing return of additional cylinders is to consider the added mass they add vs the physical mass required. The material mass of the cylinders can be approximated given some assumptions about the geometry. Here its assumed that they're made of steel (density=7850 kg/m^3) and have a thickness of 0.0375m (2.5% of the largest diameter, which is the largest value possible given a 5% decrease in diameter). Figure 21 shows the cumulative added mass of a nested cylinder system normalized by the cumulative material mass contained in those cylinders. Figure 22 shows each additional cylinder's marginal contribution to added mass and material mass. As each cylinder gets smaller, it contributes less added mass to the system but still requires a significant material mass. For the chosen thickness, the third cylinder contributes added mass that is almost half of its nominal mass. In contrast, the 15th cylinder only contributes added mass equal to 5% of its nominal mass.

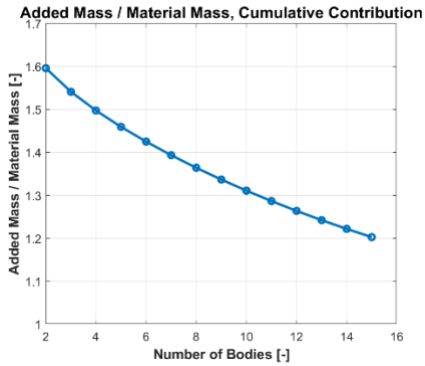

Figure 21. Cumulative contribution of added mass vs material mass.

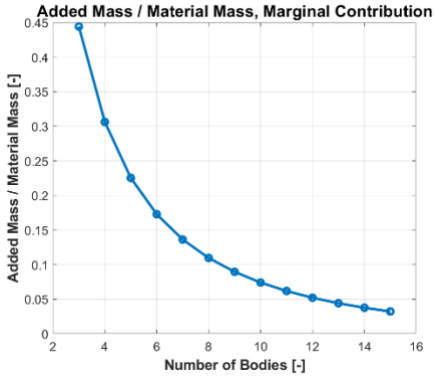

Figure 22. Marginal contribution of added mass vs material mass.

TASK 2: Development of a WEC-Sim model of the MADWEC Concept

- Task 2: Development of a WEC-Sim model of the MADWEC Concept

- *Subtask 2.1*

After completion of Task 1, UMD provided details on the geometry and mass properties of each hydrodynamic body found in the MADWEC which included a surface float, PTO chamber, and ballast system. Iterations on the mass and geometry were completed until hydrostatic balance was achieved. The final mass properties and geometric dimensions used to generate hydrodynamic coefficients are defined in Table 2-Table 5.

Table 2: Geometric and mass properties of the surface float.

Variable	Value	Unit
Height	1.25	m
Radius	0.5	m
Diameter	1.0	m
Total Volume	0.982	m3
Draft	0.82	m
Target Buoyancy	644.02	kg
Center of buoyancy	[0, 0, -0.41]	m
Target Mass	157.256	kg
Net Buoyancy	486.77	kg
Center of Gravity	[0, 0, -0.195]	m
Mass Moment of Inertia (MOI)	[30.31, 30.31, 19.66]	kg.m2
Heave Hydrostatic Spring	7,700	N.m-1
Heave Infinite Frequency Added Mass	239	kg

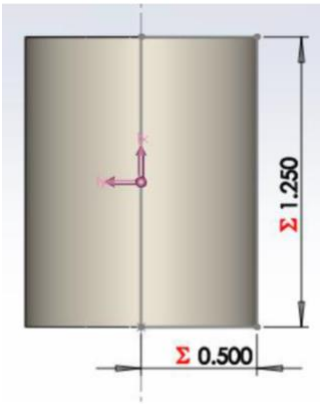

Figure 23: CAD drawing of the surface float.

Table 3: Geometric and mass properties of the PTO chamber.

Variable	Value	Unit
Height	3.7338	m
Radius	0.111125	m
Total Volume	0.145	m3
Submergence Depth (to Cg)	-53.0	m
Target Buoyancy	144.852	kg
Center of buoyancy	[0, 0, -52.6869]	m
Target Mass	111.130	kg
Net Buoyancy	33.72	kg
Center of Gravity	[0, 0, -53.0]	m
Mass Moment of Inertia (MOI)	[129.45, 129.45, 0.69]	kg.m2

Figure 24: CAD drawing of the PTO chamber.

Table 4: Geometric and mass properties of the ballast system.

Variable	Value	Unit
Cylinder Height	1.5	m
Radius	Varying	m
Total Volume	1.736	m3
Submergence Depth (to Cg)	-83.510	m
Target Buoyancy	1,731.944	kg
Center of buoyancy	[0, 0, -83.51]	m
Target Mass	2,251.59	kg
Net Buoyancy	-519.59	kg
Center of Gravity	[0, 0, -83.51]	m
Mass Moment of Inertia (MOI)	[59358,59358,866]	kg.m2
Heave Infinite Frequency Added Mass	16,260	kg

Figure 25: CAD drawing of the ballast

Table 5: Geometric parameters of the six open top cylinders used in the ballast system design.

Ballast #	Outer Radius	Inner radius	Units
1	0.75000000	0.71000000	m
2	0.70500000	0.66650000	m
3	0.67687500	0.63687500	m
4	0.64303125	0.60303125	m
5	0.61087969	0.57087969	m
6	0.58033570	0.54223570	m

Once the hydrostatic equilibrium conditions were set, the resulting immersed volumes could then be meshed and run through WAMIT to generate the hydrodynamic coefficients required to run WEC-Sim. The resulting hydrodynamic coefficients are plotted in 26 when setting the water depth to infinite as requested by UMD. All rigid body six degree of freedom coefficients were calculated; however, only the heave coefficients are shown as the WEC-Sim model described in Subtask 2.2 was constrained to oscillate in heave only. As highlighted by Figure 26, the heave added mass of the ballast system is dominant, as anticipated, and as described in Task 1 is frequency independent. The frequency independence is apparent for the PTO chamber while the surface float has stronger frequency dependence however the scaling in 26 diminishes the visual observation. The radiation wave damping

has the opposite result with the surface float having the largest damping and the PTO chamber and ballast having little to no damping. This is consistent with the submergence depth of the PTO chamber and the ballast as the deeper an object is placed in the water column the hydrodynamics are moving more towards oscillation in an infinite fluid rather than in the presence of a free surface. The combined free surface boundary condition dictates the propagating waves that radiate away from the oscillating body and therefore if no waves are generated no energy is radiated away and the damping should tend to zero. For the heave wave-excitation force the surface float continues to provide the largest values which follows a similar argument as the wave radiation damping. In deep water conditions, the wave pressure decays exponentially with wavelength resulting in minimal wave pressure penetrating deep in the water column. The ballast does have a local maximum at very long wave periods, but these are above of the 20 s range which is generally the upper limit of regularly occurring gravity wave periods.

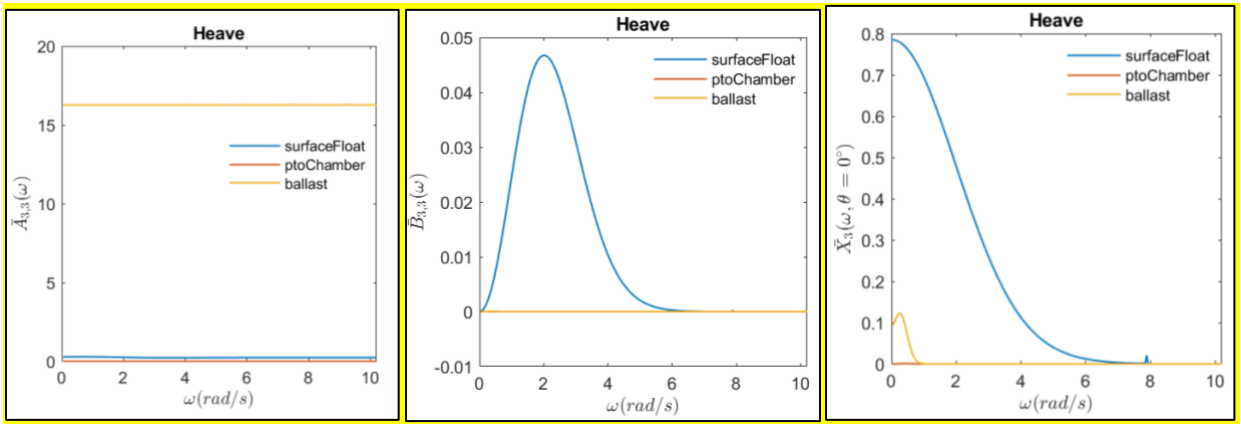

Figure 26: (Left) Heave radiation added mass, (Center) radiation wave damping, (Right) wave excitation force against wave frequency for the surface float, PTO chamber, and ballast.

The natural frequency of the multiple degrees of freedom were found to have significant impact on the device dynamics and the WEC-Sim facility completed several checks to understand how hydrodynamic and PTO properties were influencing the natural frequencies.

$$\omega_{res} = \sqrt{\frac{K_{33} + K_{PTO}}{m + \mu_{33}(\infty)}} \qquad (1)$$

where in Eqn. (1) K_{33} is the heave hydrostatic spring coefficient, K_{PTO} is the PTO spring coefficient, m is the material mass, and $\mu_{33}(\infty)$ is the infinite frequency heave added mass. The only term not dependent on geometry or material selection, is the PTO spring coefficient which can be selected by UMD. If a PTO spring coefficient of 1,000 N/m is assumed, for the time being, the natural period of just the surface float is 1.34 s. Based on Eqn. (1) we can see that for any larger PTO spring the natural period will decrease and for most wave conditions the surface float will act as a wave follower.

Further discussion will be provided under Subtask 2.2 reporting, but the resonant period for the ballast attached to the same PTO spring provides another natural frequency to the system. If one considers the PTO spring to be attached to a stationary reference at the still water line, then the ballast has no hydrostatic stiffness which results in a natural period of 27 s. The team also calculated the natural period if there was no added mass, UMD's concept transitions between full and no added using their openings on the bottom of the open top cylinders, which came out to be 9.38s. An interesting finding

from the WEC-Sim runs with bidirectional added mass was that because the cylinder bottoms open and close twice during the wave cycle the simulation is being excited at the wave frequency and twice the wave frequency. This means that if the resonance period is half the current wave period, excessive motion can be triggered which highlights the importance of selecting the PTO spring coefficient along with the geometric and mass properties of all the hydrodynamic bodies.

- *Subtask 2.2*

Base WEC-Sim Model Development

With mass properties and hydrodynamic coefficients obtained, a WEC-Sim model can be built and used to simulate various configurations of the MADWEC. The first step in the model building process was to construct the Simulink model of the MADWEC system, as shown in 27. The Simulink model consists of 7 major objects which includes three hydrodynamic bodies (yellow blocks), a sea floor reference (green block), two constraints (clear blocks), and one power take-off (PTO) (grey block) which can all be obtained from the default WEC-Sim Simulink Library. A translational constraint is connected between the ballast and the sea floor to restrict motion to heave only. In the MADWEC design, Figure 2, the connection between the ballast and the PTO chamber could be either cables or a rigid bar but UMD and the WEC-Sim facility agreed to start with a rigid connection which allows the WEC-Sim model to utilize a fixed constraint between the ballast and PTO chamber locking the motion of the two bodies together. A translational PTO, oriented vertically, acts as the connection between the surface float and the PTO chamber as the relative motion between these two hydrodynamic bodies is the input to the PTO. Once the Simulink model was built the corresponding *wecSimInputFile.m* could be written, see 28, which is used to define the sea conditions, mass properties, and PTO properties. For brevity, descriptions of the object classes will not be discussed but interested readers can review the WEC-Sim documentation to understand all of WEC-Sim's acceptable inputs.

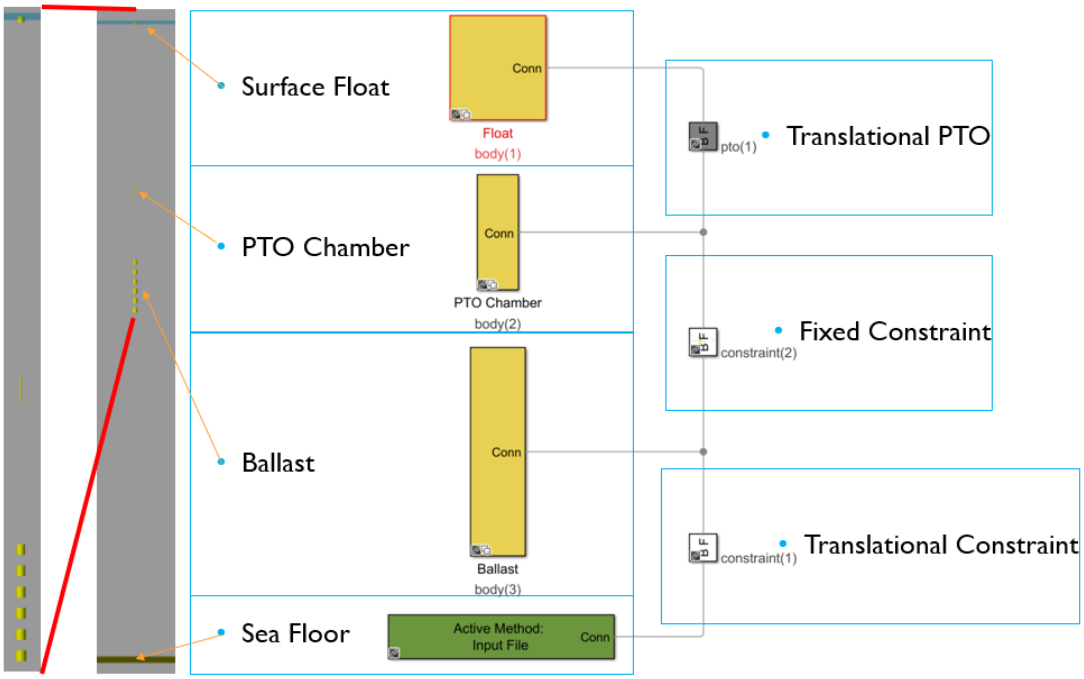

Figure 27: MADWEC WEC-Sim Simulink Model highlight the hydrodynamic bodies, seafloor, PTO, and constraints.

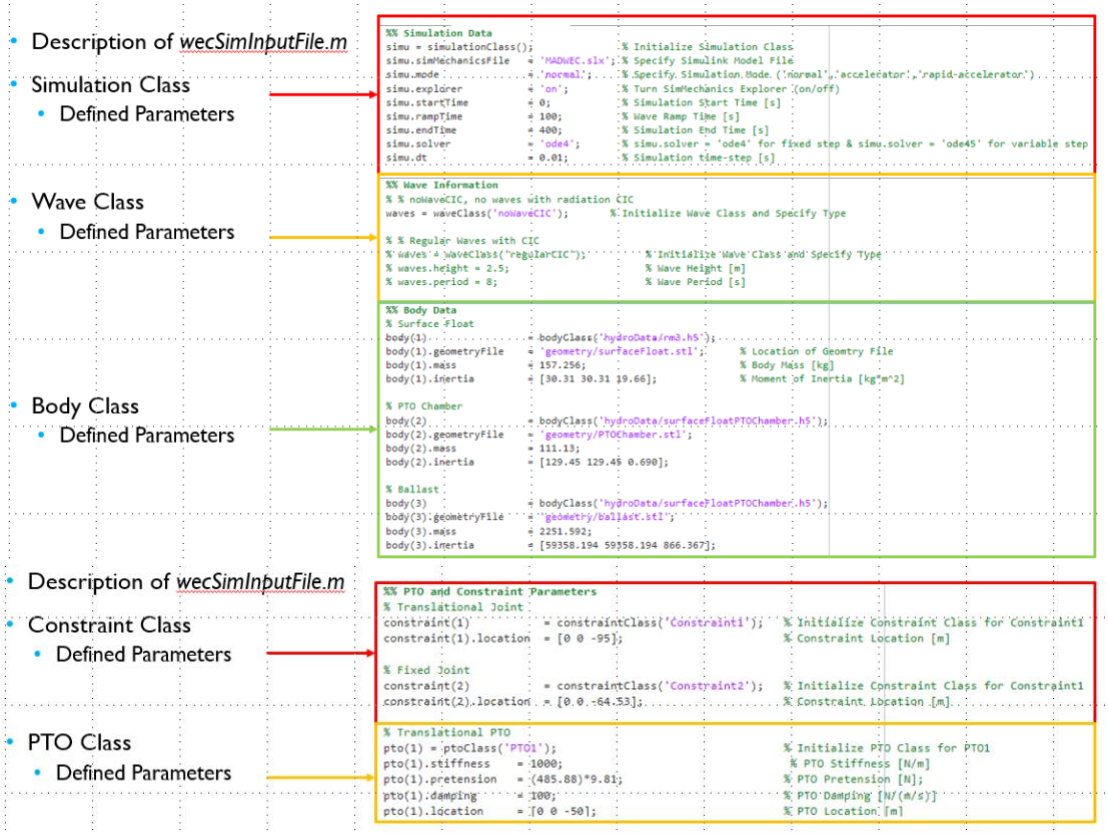

Figure 28: MADWEC WEC-Sim "wecSimInputFile.m" listing inputs to run a calm water 'noWaveCIC' simulation.

Bidirectional Added Mass Implementation

A novel hydrodynamic feature of the MADWEC system is the inclusion of the louvers in the bottom of the open top cylinders which results in changing or variable added mass based on the direction of motion. Once the base WEC-Sim model was built, the next step was to create custom function that would allow the model to account for the variable bidirectional added mass. The bidirectional added mass is implemented in Simulink and MATLAB. The ballast body is unlinked from the WEC-Sim library to be modified (Figure 29**Error! Reference source not found.**). The 'Geometry Variation' block (Figure 29**Error! Reference source not found.**) is added and sends the relevant hydrodynamic forces (excitation force, added mass force and radiation damping force), ballast velocity and mass information to a MATLAB function "ballastVariation". This function checks when the ballast velocity changes sign and scales the forces as needed. When the ballast is fully closed forces remain as is, based on the closed-ballast BEM coefficients. When the ballast is fully open forces are scaled by a specific factor in each degree of freedom. These scaling factors were determined by comparing the BEM results of an open ballast system and a closed ballast system (closed louvers, the top of the cylinders are still open). The detailed BEM comparison between these cases is shown in the appendix. The scaling factors chosen for each force and degree of freedom are taken to be:

$$R_{excitation} = \frac{F_{open}}{F_{closed}} = [0.9 \;\; 0.0 \;\; 0.06 \;\; 0.0 \;\; 1.0 \;\; 0]$$

$$R_{radiation\ damping} = \frac{F_{open}}{F_{closed}} = [0.8\ \ 0.8\ \ 0.00\ \ 1.0\ \ 1.0\ \ 0]$$

$$R_{added\ \ mass} = \frac{F_{open}}{F_{closed}} = [0.9\ \ 0.9\ \ 0.01\ \ 0.9\ \ 0.9\ \ 0]$$

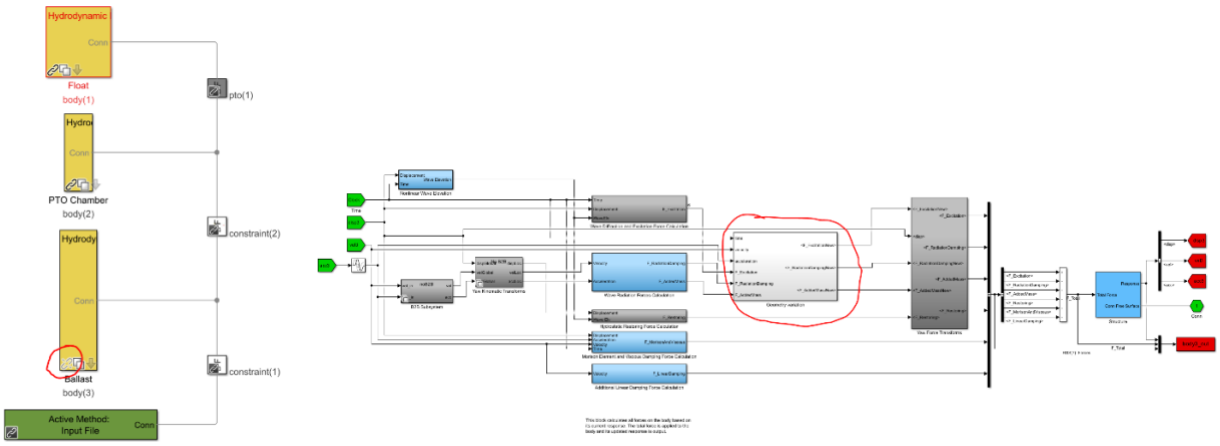

Figure 29: Simulink diagrams showing where the custom hydrodynamic functionality is implemented. Ballast body unlinked from the WEC-Sim library (left) and additional function added to the body (right). Changes circled in red.

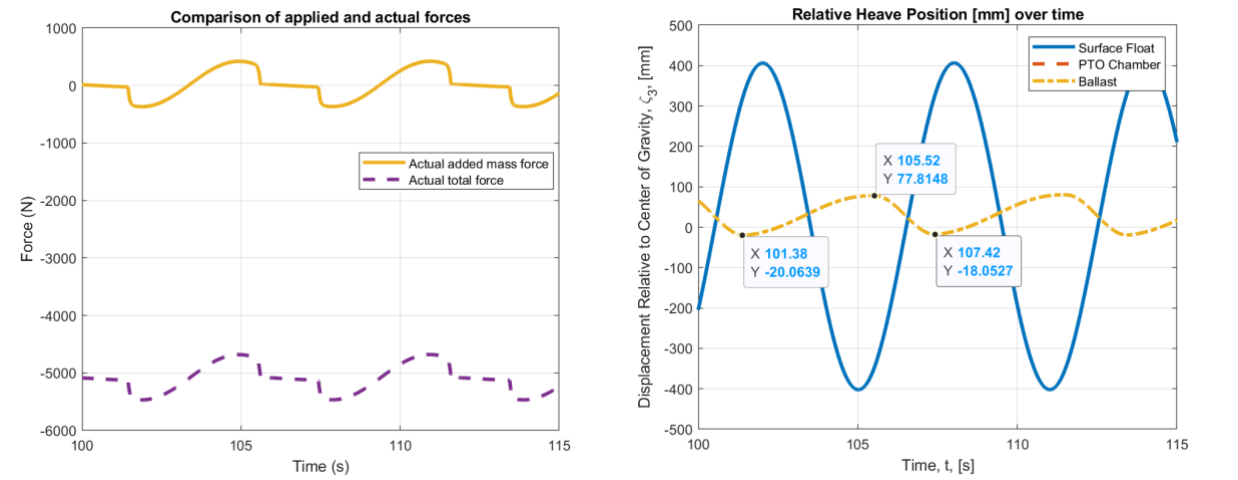

Figure 30: (Left) Relative heave position of the bodies over time and (Right) actual added mass force and total forces applied to the body during simulation.

The hydrodynamic variation also includes a ramp function to represent the real transition time when louvers are dynamically opening or closing. The ramp function is identical to those applied elsewhere in WEC-Sim. Its form is sinusoidal and ramps both smoothly and continuously between the closed ballast forces and the open ballast forces. The transition time is taken to be 0.2 seconds, based on prior work at the University of Massachusetts Dartmouth. Readers should note that special attention must be paid to WEC-Sim's added mass implementation when altering the added mass force during the simulation itself.

Figure (Left) shows the results of a sample WEC-Sim simulation when only the bidirectional hydrodynamics are considered. This case uses a regular wave with a 1 meter height and 6 second

period. Figure (Right)Figure 31 shows that, as expected, the bidirectional added mass results in the ballast system ascending slowly and descending quickly over a single wave period. The ballast period is still equivalent to the wave period (6 seconds here), but motion is more heavily weighted on the upstroke. The ascent lasts approximately 4 seconds or 2/3 of the wave period, while the descent is only 2 seconds or 1/3 of the wave period. The surface float position continues to follow the wave elevation. Figure 31 shows how the heave added mass force and heave total force on the ballast change as the louvers open and close. There is a clear demarcation where the added mass force significantly increases and decreases in amplitude when the ballast velocity changes sign.

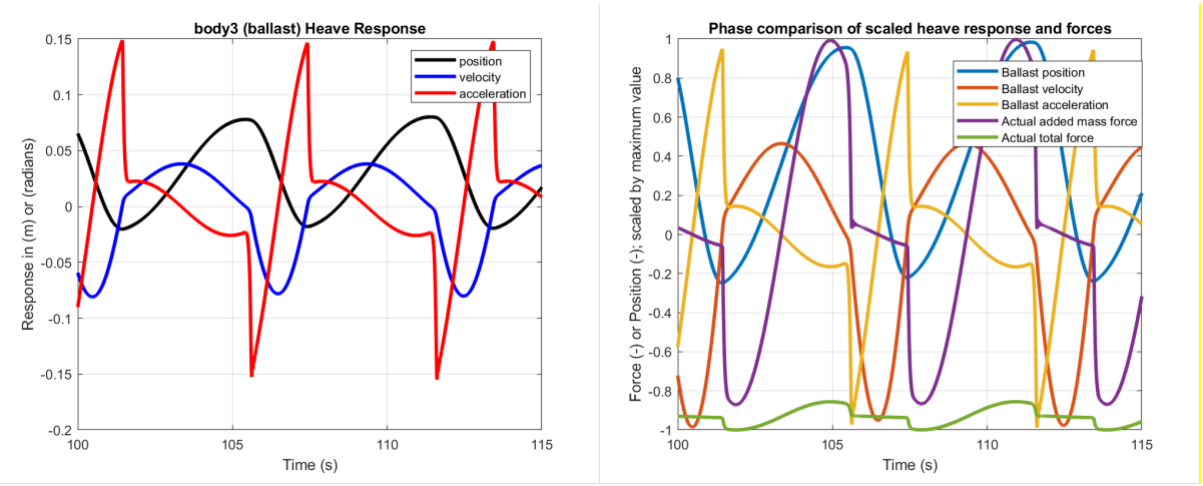

Figure 31: (Left) Heave response of the ballast and (Right) heave response and forces, scaled by their maximum value to compare the phase of each over time.

Figure 3131 shows a different method of visualizing the bidirectional added mass effects. Figure 31 shows how the velocity changing sign results in an immediate change in the magnitude of the acceleration (via the added mass force). When the velocity changes from negative to positive, the louvers close, increasing the added mass force which increases resistance to device motion, which decreases the acceleration. The opposite effects happen when the velocity changes sign to negative and the louvers open. Figure 3131 (Right) combines the comparisons of Figure 30 and Figure 3131 (Left). It shows the relevant heave forces and motion of the ballast together. Quantities are scaled to a fraction of their maximum value so that phase information can be more easily compared.

- *Subtask 2.3*

Simplified Bidirectional PTO model

The MADWEC PTO design includes a one-way clutch which results in a damping force, and power generation, to be active only with vertical motion on the upstroke. To model this effect, the Translational PTO used in the base WEC-Sim model needed to be replaced by a Translational PTO Actuation Force block, shown in Figure 32432, which allows the user to define the force implemented by the PTO block based on whatever parameters or signals required. Figure 33 shows the calculation of the PTO force based on the instantaneous position and velocity of the relative motion between the surface float and PTO chamber. The PTO control law here is similar to a proportional and integral controller, but the proportional law is only active on the upstroke to represent the MADWEC's one way clutch.

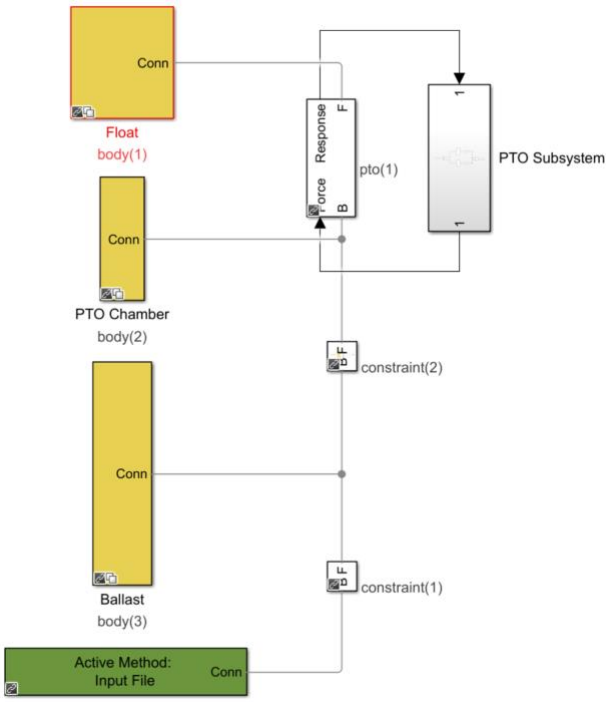

Figure 324: MADWEC Simulink model with Translational PTO Actuation Force block and PTO Subsystem.

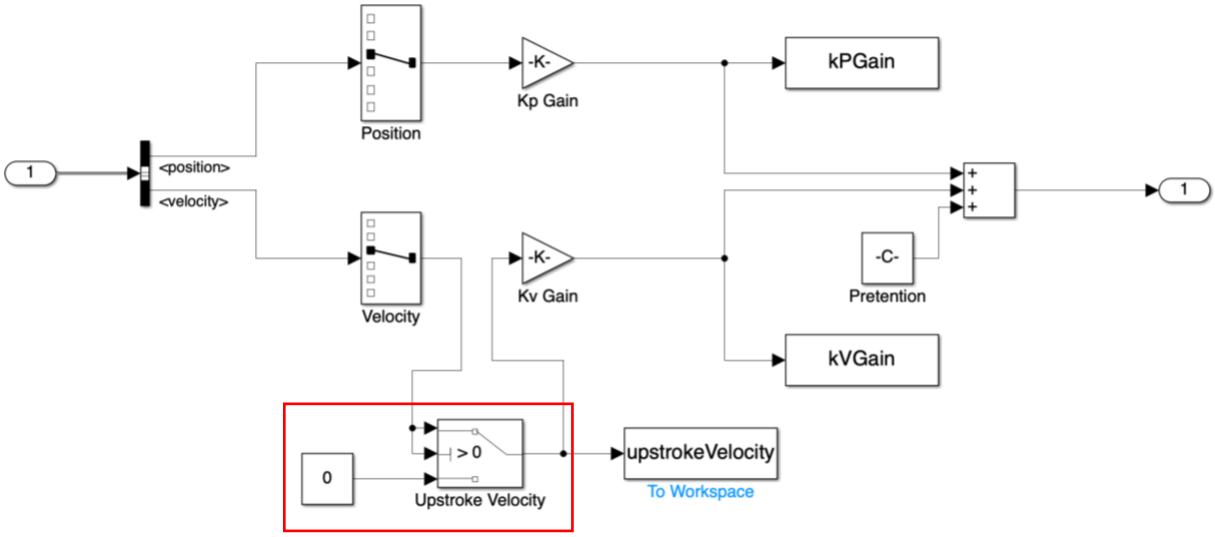

Figure 33: Simulink operations within the PTO Subsystem which implements damping force only on the upstroke.

UMD Custom PTO Model Incorporation

The simplified bidirectional PTO model clarified the influence of the global response of the system to a one-way clutch implementation. During this process UMD had been refining a PTO model based on components specifications and results obtained from dry bench top testing. The model was built within Simulink which allowed the WEC-Sim facility to swap out the PTO Subsystem components shown in Figure 33 with those shown in Figure 34 and Figure 35. The WEC-Sim facility needed to make minor adjustments to the model to be consistent with the WEC-Sim coordinate system and reduce start up

transients. After receiving initial performance metrics based on the custom PTO model, UMD provided another custom PTO model which will be denoted as Version 1 and Version 2 for the rest of this report.

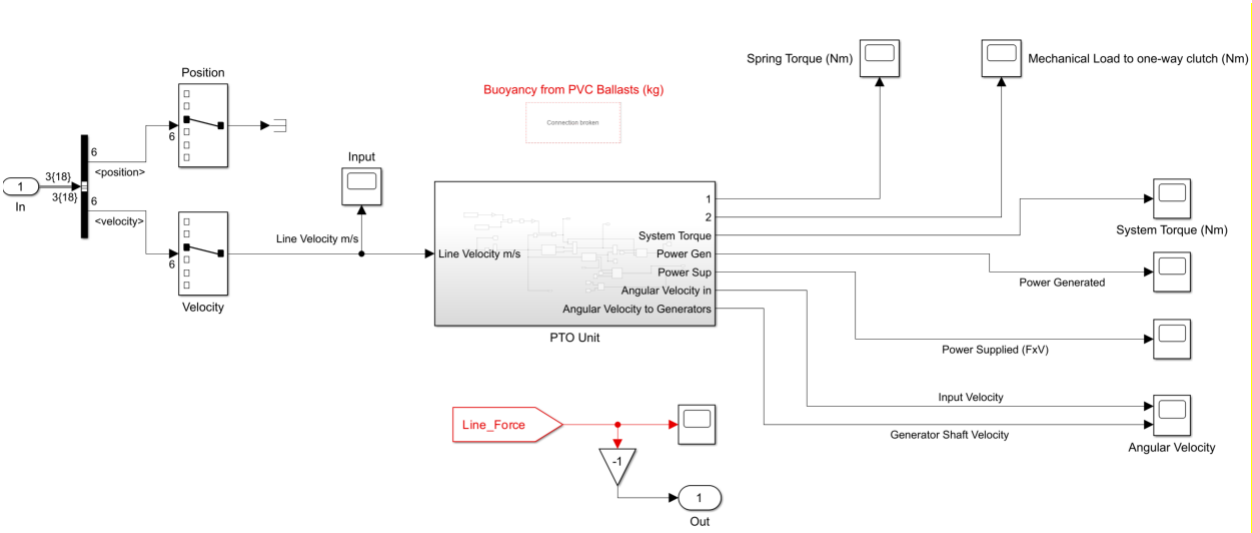

Figure 34: Top level within PTO Subsystem based on the UMD Design

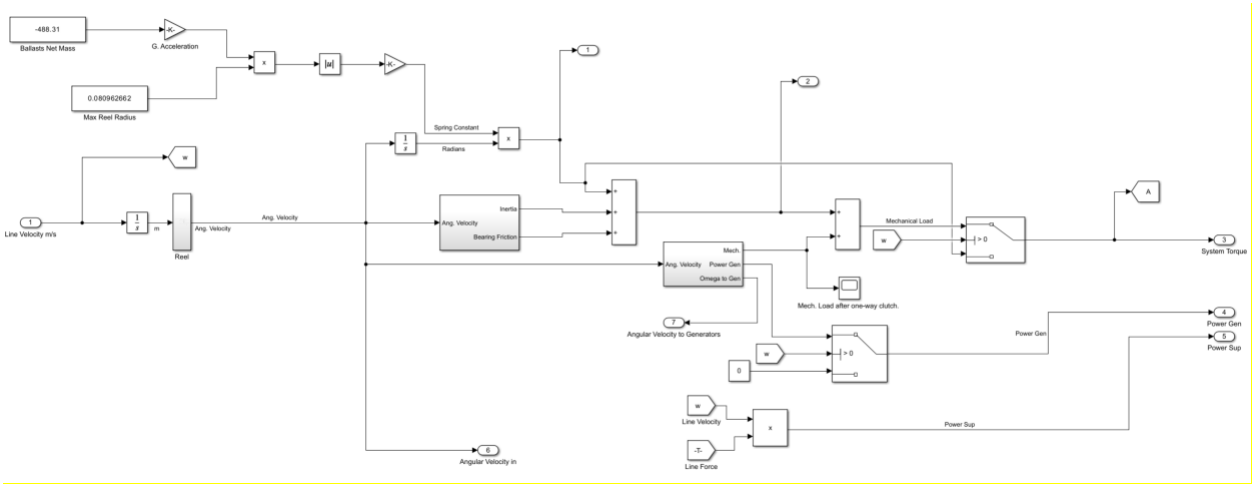

Figure 35: Simulink model found under the "PTO Unit" shown in Figure .

- *Subtask 2.4*

Calm Water to test hydrostatic stability

The WEC-Sim facility always recommends building up the environmental conditions (i.e. wave conditions) to verify all forcing within the model is acting properly. The first step is to deploy the model in a calm (static) water condition to ensure hydrostatic stability. If the model has been developed properly the device should remain approximately stationary at the deployed positions. As shown in Figure 36, there may still be small transients as a result of slight force imbalances but these oscillations are extremely minimal and more importantly do not become unstable. Several model configurations were tested to verify that the mass and buoyancy calculations were accurate (i.e. device did not sink or

rise above the calm water surface) and that will small oscillations the hydrostatic restoring matrix continued to bring the model back towards the equilibrium condition.

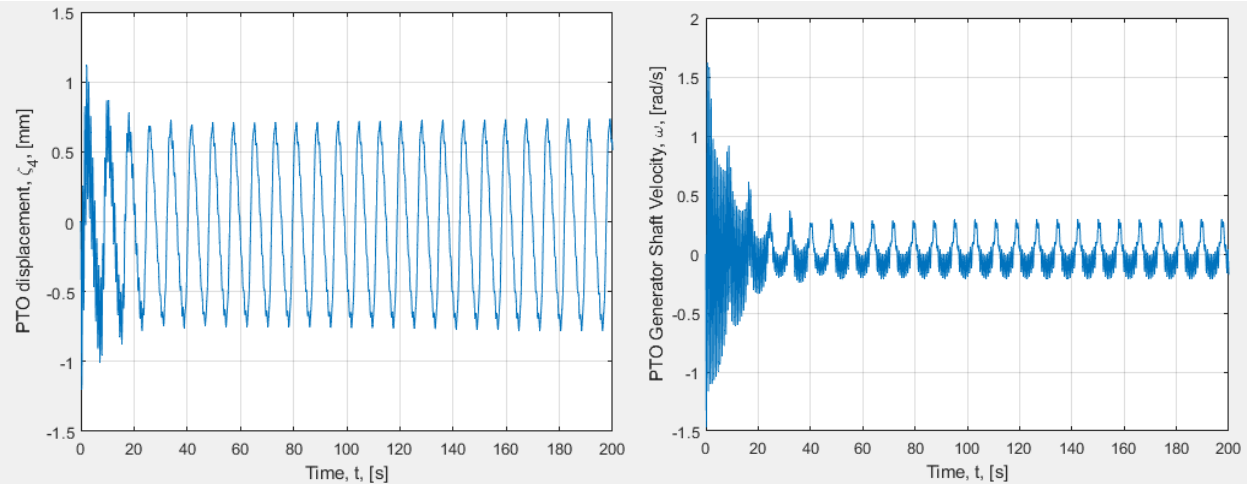

Figure 36: (Left) Time history of the PTO displacement and (Right) time history of the PTO generator shaft velocity. Both plots illustrate a minimal initial transient which quickly decays to small amplitude oscillation about the mean positions.

Free Decay to test radiation and hydrostatic coefficients

After completing the no wave test, a free decay test was conducted by displacing the surface float out of the water by 0.1 m. The initial PTO displacement in the UMD custom PTO model also needed to be updated to reflect this initial displacement. The corresponding time histories of motion, Figure , and PTO torque and power, Figure 37, follow a decaying trend as desired and if the time was extended indefinitely all signals should decay to zero. Such a performance indicates that the dissipative mechanisms are active in the model and should help reduce the potential for unstable behavior. A unique result, highlighted in Figure 37 , is the multiple harmonics excited in the decay. At the beginning the surface float has much faster oscillations tied to its natural response, but since the surface float has greater radiative damping the oscillations decay and align with the motion of the PTO chamber + ballast. The longer oscillation period is tied to the natural period of the lower bodies with the PTO stiffness and because of the very low wave damping and PTO damping the oscillations have minimal decay and recovers the response of a mass-spring system.

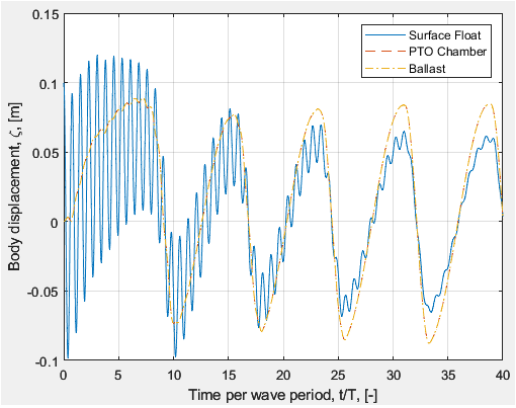

Figure 37: Hydrodynamic body displacements during a free decay test by initially displacing the surface float up by 0.1 m.

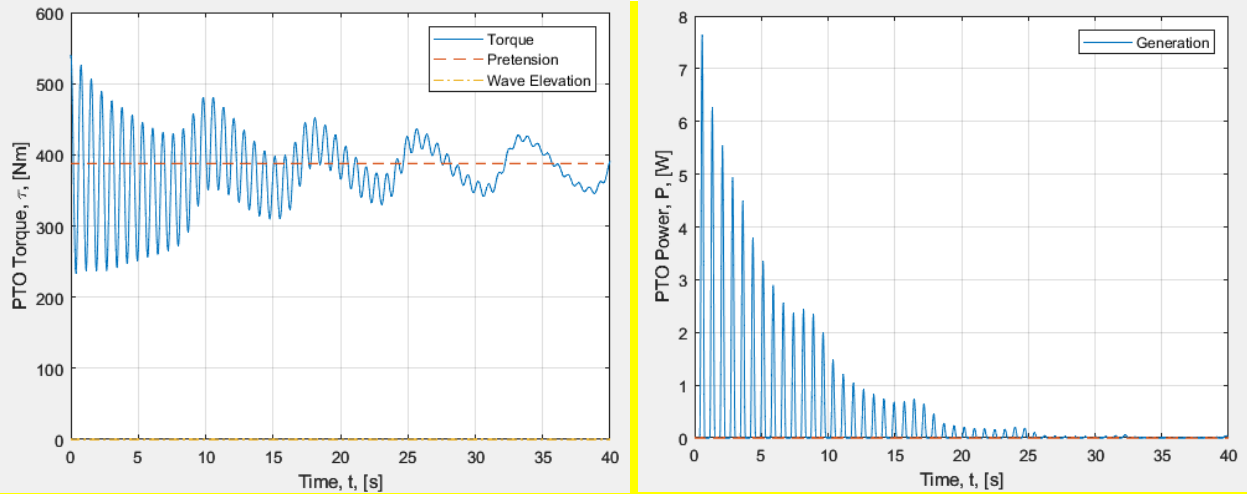

Figure 38: (Left) PTO torque and (Right) PTO generated power time histories from a free decay test by initially displacing the surface float up by 0.1 m.

Regular Wave Runs with several wave heights over a vector of wave periods

The next step in the simulation process was to move to regular waves where the custom PTO models and the bi-directional added mass implementation could be evaluated. The first simulations started with smaller wave amplitudes to align more closely with linear hydrodynamic theory before ramping up the wave amplitude that would highlight any nonlinearities in the model. Sample results from a regular wave simulation for the same wave period but varying wave heights is shown in **Error! Reference source not found.**39 and Figure 40. The PTO displacement was normalized by the wave height to estimate nonlinear behavior, but at least for this wave period the response is linearly proportional to the wave height while the generated power is approximately 100 times greater which is consistent with power scaling with the square of the wave amplitude.

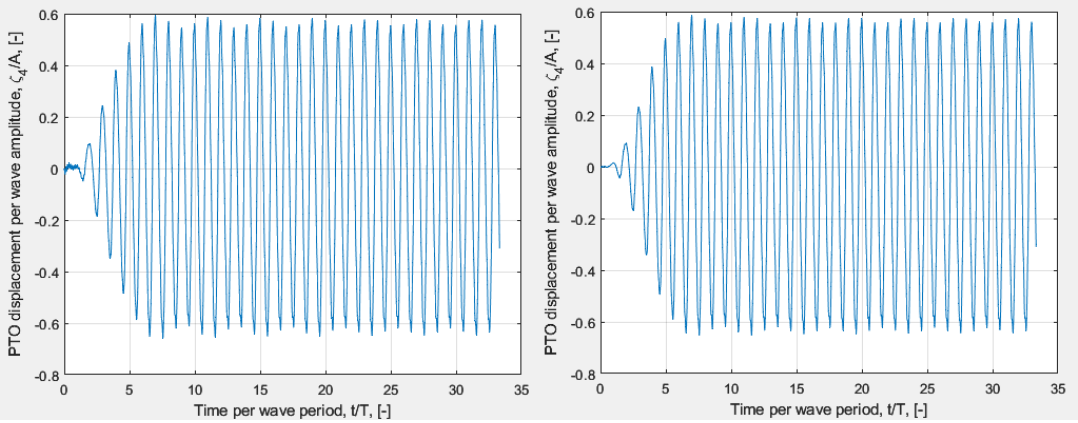

Figure 395: (Left) PTO displacement for a wave height of 0.1 m and (Right) with a wave height of 1.0 m.

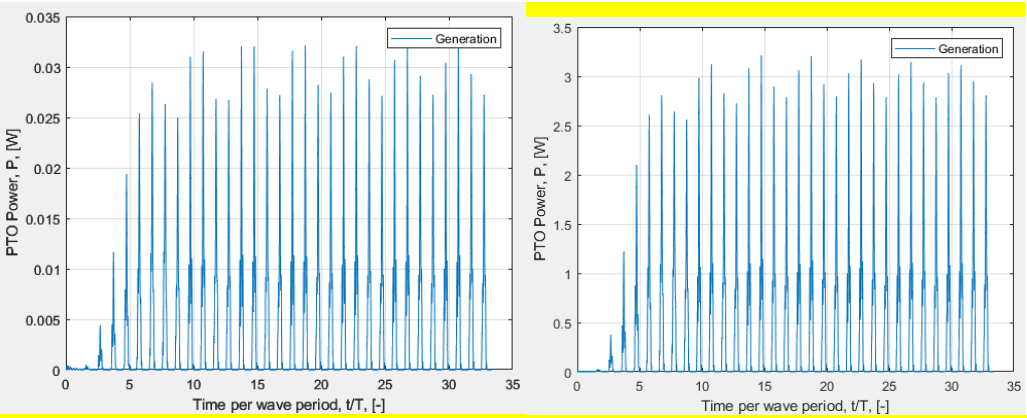

Figure 40: (Left) Power generated from UMD PTO model for a wave height of 0.1 m and (Right) with a wave height of 1.0 m.

The results in Figure 41641 and Figure 42 illustrate the time history response of the MADWEC at different wave frequencies. The project team would like to highlight the time histories as the bi-directional added mass implementation was a key component of this award and would not be highlighted from a traditional frequency domain response amplitude operator. A key characteristic in these plots is the clear indication of a secondary harmonic in the response that is tied to the opening and closing of the ballast flaps. Under regular wave excitation, approximately half of the wave cycle the ballast will have near zero added mass which impacts the ballast acceleration resulting in different rise and fall times that is reflected in additional harmonics in the time histories. The project team would also like to acknowledge that the normalized response, relative to the wave amplitude, has a rather large amplification that might begin breaking the assumptions of the linear hydrodynamic theory used to model the MADWEC system. However, after checks both in the time and frequency domain these amplitudes were traced back to the PTO stiffness, PTO damping, and total added mass of the ballast. Further discussion on these lessons learned can be found in Section 7.2.

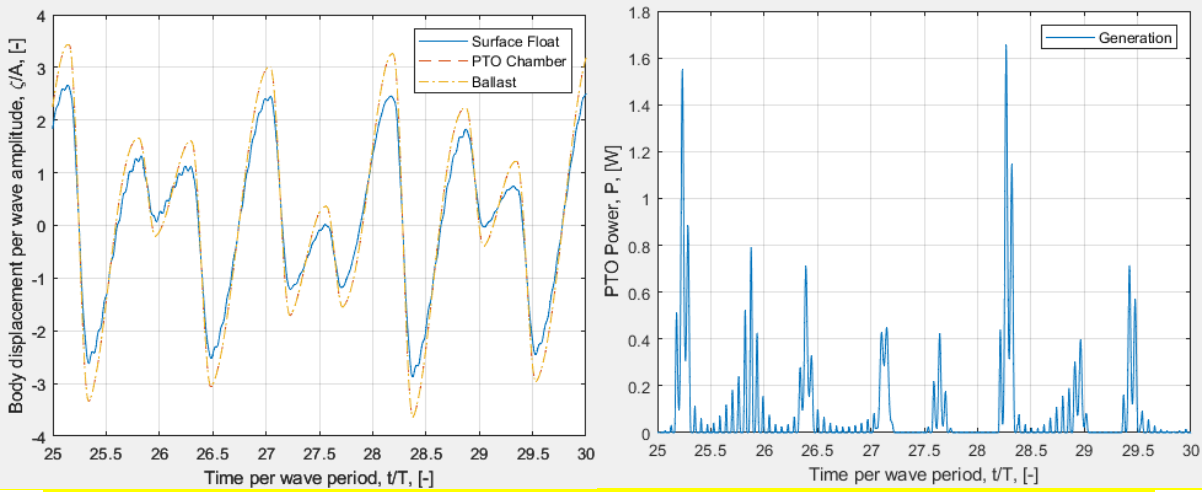

Figure 416: Time histories from a WEC-Sim run using regularCIC, a wave period of 13 s, and a wave height of 0.5 m.

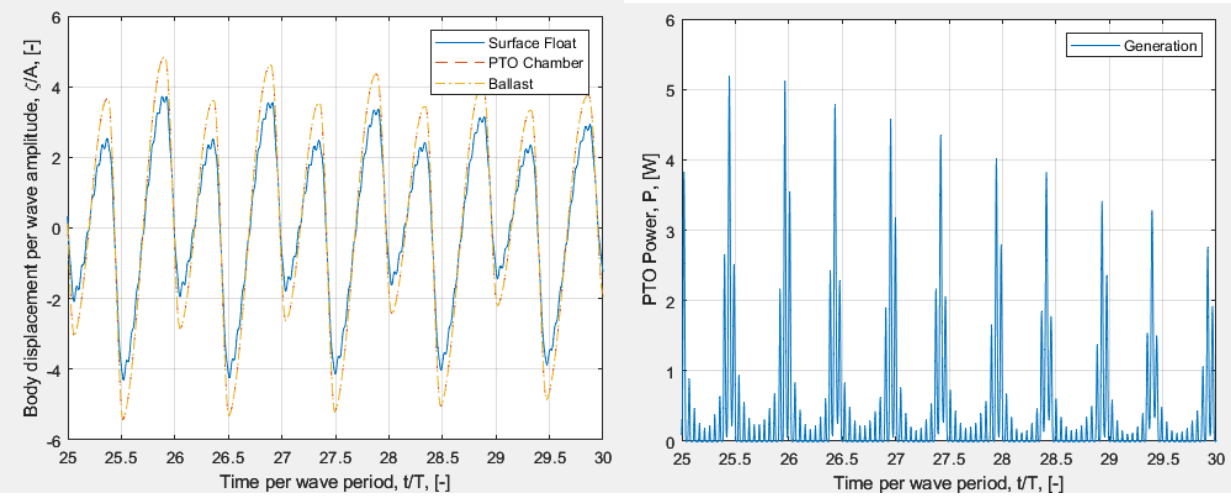

Figure 42: Time histories from a WEC-Sim run using regularCIC, a wave period of 16 s, and a wave height of 0.5 m

Power Matrix to obtain initial estimates on realistic power production

After UMD understood the performance of the model in regular waves and chose to move forward with generating initial power matrices, a series of wave heights and wave periods that were representative of the New England cost were provided to the WEC-Sim team as follows:

- Wave heights:
  - 0.38, 0.66, 0.96, 1.25, 1.50, 1.75, 2.00, 2.50, 3.00 m
- Wave Periods:
  - 4, 5, 6, 7, 8, 10, 11, 12, 14, 16, 18 s

which results in 99 combinations of wave height and wave period. Prior to running irregular waves, these combinations of wave height and period were run under regular waves. The simulations were run with a ramp time of 20*T_p and a total simulation time of 70*T_p. The min, max, mean, and standard deviation metrics where then calculated over a period of 50 peak period wave cycles and for a range of model parameters. The amount of data collected was significant and will be uploaded to MHKDR, but for this report sample plots will be shown for brevity. The results for power generation across the combination of sea states is shown in Figure 43-Figure46, where the average power generation between PTO Version 1 and Version 2 is about 10 orders of magnitude larger. The reason for this discrepancy was that PTO Version 1 provided very little damping compared to the optimum PTO damping for maximum power extraction. PTO Version 2 was redesigned to have a larger sized electric generator, although still below optimum, to provide a greater damping force that resulted in much greater power absorption.

Next, the same batch runs were then simulated using irregular waves using a Pierson-Moskovitz spectrum with the same ramp and total simulation times used in the regular wave cases. The results from these simulations are shown in Figure 47747 and Figure 48 that illustrate the influence of having a polychromatic rather than a monochromatic sea state. The major takeaways from the irregular wave sea states are that the polychromatic seas with bi-directional added mass appear to be more sensitive to the incident wave train as although there is a general trend in improving power performance with increasing wave height there is much greater scattering in average power. The previous results from the RAO task did identify wave frequencies that resulted in resonance conditions which likely were easier to avoid in

regular waves, but because of energy spreading across multiple frequencies in irregular seas, these resonances might be triggered more frequently resulting in the increased scatter in results.

Instantaneous Power Generated Mean [W]													
	# Cases	1	2	3	4	5	6	7	8	9	10	11	simu.endTime
# Cases	Hs/Tp	4	5	6	7	8	10	11	12	14	16	18	
1	0.38	0.000943	0.000944	0.001284	0.004224	0.005984	0.000572	0.000291	0.000221	0.000192	0.000519	0.000123	
2	0.66	0.002727	0.002535	0.003857	0.012604	0.018292	0.001706	0.000888	0.000621	0.00058	0.0016	0.000395	
3	0.96	0.005485	0.005096	0.008138	0.02651	0.039004	0.003604	0.00189	0.001336	0.001205	0.003397	0.000814	
4	1.25	0.009075	0.00847	0.013801	0.04478	0.066319	0.00613	0.0032	0.002299	0.002019	0.005747	0.001369	
5	1.50	0.01309	0.012079	0.01984	0.064661	0.0956	0.008816	0.004607	0.003326	0.002892	0.008288	0.001964	70*Tp
6	1.75	0.017414	0.016394	0.027007	0.0878	0.130268	0.011989	0.006276	0.004542	0.003934	0.011246	0.00266	
7	2.00	0.020516	0.021305	0.03528	0.114652	0.170226	0.015715	0.008217	0.005941	0.005131	0.014666	0.00347	
8	2.50	0.029595	0.033271	0.055121	0.179108	0.266385	0.024522	0.012828	0.009313	0.008	0.022798	0.005402	
9	3.00	0.040078	0.047822	0.079381	0.257783	0.383847	0.035252	0.018481	0.013422	0.011487	0.032554	0.007773	

Figure 43: Matrix of mean generated power under regular wave sea states using Version 1 of UMD's PTO model and the base of the WEC-Sim model.

Instantaneous Power Generated Max [W]													
	# Cases	1	2	3	4	5	6	7	8	9	10	11	simu.endTime
# Cases	Hs/Tp	4	5	6	7	8	10	11	12	14	16	18	
1	0.38	0.013645	0.021089	0.025502	0.094902	0.151826	0.021598	0.011102	0.007332	0.009914	0.024976	0.003351	
2	0.66	0.046354	0.045939	0.075799	0.287579	0.462227	0.066962	0.034406	0.02451	0.030005	0.080071	0.015844	
3	0.96	0.103503	0.083219	0.159857	0.602915	0.983115	0.141987	0.073474	0.057904	0.061292	0.170641	0.034909	
4	1.25	0.181572	0.130079	0.270621	1.032236	1.666014	0.242098	0.124457	0.10097	0.101231	0.289458	0.057827	
5	1.50	0.287256	0.179459	0.388349	1.491417	2.39768	0.348009	0.179111	0.145645	0.143768	0.417	0.082921	70*Tp
6	1.75	0.390797	0.239707	0.529157	2.011924	3.280071	0.473922	0.244234	0.197987	0.195347	0.567148	0.112318	
7	2.00	0.354644	0.303475	0.689395	2.640471	4.275325	0.623224	0.320966	0.25764	0.254177	0.739961	0.14645	
8	2.50	0.49799	0.472217	1.077647	4.146127	6.68315	0.970378	0.500169	0.400507	0.394677	1.150908	0.227426	
9	3.00	0.628226	0.670696	1.550218	5.9473	9.662639	1.396834	0.721473	0.569178	0.564193	1.64979	0.328525	

Figure 44: Matrix of Max generated power under regular wave sea states using Version 1 of UMD's PTO model and the base WEC-Sim model.

Instantaneous Power Generated Mean [W]													
	# Cases	1	2	3	4	5	6	7	8	9	10	11	simu.endTime
# Cases	Hs/Tp	4	5	6	7	8	10	11	12	14	16	18	
1	0.38	0.010244	0.008751	0.014079	0.044597	0.063208	0.005739	0.003038	0.002202	0.002015	0.004308	0.001263	
2	0.66	0.02938	0.025804	0.042331	0.133204	0.193231	0.017226	0.00929	0.006588	0.005954	0.013091	0.003854	
3	0.96	0.057964	0.054214	0.089586	0.281064	0.411242	0.036442	0.019763	0.013967	0.012437	0.027699	0.008121	
4	1.25	0.096211	0.091652	0.151269	0.475847	0.698921	0.061917	0.033578	0.02369	0.021006	0.046928	0.013722	
5	1.50	0.135667	0.132029	0.217838	0.685048	1.00761	0.089115	0.048314	0.034092	0.030151	0.067415	0.019692	70*Tp
6	1.75	0.178043	0.179371	0.296687	0.92976	1.372344	0.121228	0.065839	0.046405	0.040902	0.091599	0.026816	
7	2.00	0.222881	0.234293	0.387541	1.217174	1.793508	0.158248	0.086204	0.060577	0.053419	0.11947	0.034998	
8	2.50	0.324665	0.365949	0.604218	1.896544	2.805908	0.247025	0.134532	0.094776	0.083208	0.185857	0.05471	
9	3.00	0.444956	0.527253	0.87026	2.73534	4.042508	0.356255	0.194015	0.136613	0.119529	0.266761	0.078734	

Figure 45: Matrix of mean generated power under regular wave sea states using Version 2 of UMD's PTO model and the base of the WEC-Sim model.

Instantaneous Power Generated Max [W]													
	# Cases	1	2	3	4	5	6	7	8	9	10	11	simu.endTime
# Cases	Hs/Tp	4	5	6	7	8	10	11	12	14	16	18	
1	0.38	0.141316	0.13682	0.245504	0.961035	1.596479	0.168223	0.090591	0.056731	0.083164	0.154299	0.034829	
2	0.66	0.396557	0.379831	0.733748	2.871288	4.858677	0.503058	0.285293	0.211551	0.238788	0.48166	0.116064	
3	0.96	0.835521	0.782837	1.546912	6.085284	10.32188	1.058546	0.612627	0.457098	0.488635	1.025941	0.241377	
4	1.25	1.513914	1.31185	2.600014	10.34489	17.53008	1.802256	1.045675	0.767908	0.81906	1.742585	0.406775	
5	1.50	2.401286	1.887515	3.739938	14.90131	25.26348	2.601522	1.504231	1.094699	1.168219	2.513248	0.582617	70*Tp
6	1.75	3.244479	2.559399	5.09958	20.1665	34.40164	3.529586	2.056152	1.478651	1.574805	3.422235	0.79312	
7	2.00	3.950273	3.342347	6.663629	26.46743	44.93805	4.603108	2.694824	1.917958	2.054909	4.47361	1.035248	
8	2.50	5.344528	5.214805	10.37185	41.19678	70.37157	7.17653	4.203836	2.985115	3.18263	6.984835	1.613285	
9	3.00	6.66485	7.514336	14.9252	59.61003	101.3708	10.31721	6.083593	4.268568	4.549159	10.05848	2.322271	

Figure 46: Matrix of Max generated power under regular wave sea states using Version 2 of UMD's PTO model and the base WEC-Sim model.

Instantaneous Power Generated Mean [W]													
	# Cases	1	2	3	4	5	6	7	8	9	10	11	simu.endTime
# Cases	Hs/Tp	4	5	6	7	8	10	11	12	14	16	18	
1	0.38	0.000129	0.000191	0.000117	0.002076	0.001462	0.000269	0.001256	0.000549	0.00051	0.000297	0.000154	
2	0.66	0.00053	0.000927	0.003522	0.002168	0.008133	0.008533	0.007893	0.00413	0.000573	0.006631	0.000401	
3	0.96	0.001506	0.002911	0.005009	0.005741	0.015623	0.003616	0.009434	0.007681	0.004751	0.002616	0.005826	
4	1.25	0.003831	0.002704	0.009238	0.008996	0.004648	0.009631	0.036963	0.02169	0.005375	0.003026	0.005743	
5	1.50	0.007526	0.003818	0.009527	0.038678	0.009296	0.0139	0.007811	0.003451	0.022812	0.004508	0.00325	70*Tp
6	1.75	0.00402	0.007086	0.007596	0.007413	0.057871	0.01484	0.028421	0.004977	0.015718	0.029657	0.03292	
7	2.00	0.003645	0.012456	0.010398	0.009748	0.014757	0.019829	0.026774	0.016461	0.027564	0.01443	0.014769	
8	2.50	0.018774	0.032885	0.029492	0.051833	0.028731	0.025652	0.091744	0.097951	0.014034	0.013579	0.023568	
9	3.00	0.007815	0.018394	0.011806	0.047379	0.085405	0.052147	0.42889	0.052225	0.066095	0.043073	0.011473	

Figure 477: Matrix of mean generated power under irregular wave sea states using Version 1 of UMD's PTO model and the base of the WEC-Sim model.

Instantaneous Power Generated Mean [W]													
	# Cases	1	2	3	4	5	6	7	8	9	10	11	simu.endTime
# Cases	Hs/Tp	4	5	6	7	8	10	11	12	14	16	18	
1	0.38	0.003036	0.006049	0.001088	0.00549	0.020591	0.019443	0.008042	0.00749	0.002835	0.002668	0.004846	
2	0.66	0.007769	0.006167	0.02272	0.009332	0.054119	0.003379	0.029278	0.053189	0.030065	0.023932	0.016466	
3	0.96	0.022795	0.024966	0.132466	0.12071	0.033012	0.129214	0.03586	0.158931	0.081228	0.066792	0.020868	
4	1.25	0.018739	0.115035	0.015445	0.029467	0.085344	0.089064	0.094597	0.10241	0.06454	0.207715	0.021866	
5	1.50	0.039916	0.054448	0.190615	0.023107	0.069491	0.068761	0.10736	0.230543	0.143006	0.078172	0.192265	50*Tp
6	1.75	0.048222	0.123947	0.113683	0.084003	0.228062	0.503356	0.311586	0.38959	0.570991	0.045516	0.087768	
7	2.00	0.062825	0.036858	0.198914	0.800991	0.145134	0.104846	0.116741	0.231596	0.030341	0.360732	0.093605	
8	2.50	0.100893	0.341991	0.187534	0.32578	0.307892	2.500008	0.559601	0.308136	0.667323	0.500075	0.07244	
9	3.00	0.104811	0.197459	0.43835	0.348864	0.359108	0.322516	2.435393	2.259933	0.503437	0.100063	0.626891	

Figure 48: Matrix of mean generated power under irregular wave sea states using Version 2 of UMD's PTO model and the base of the WEC-Sim model.

7.2 Lesson Learned and Test Plan Deviation

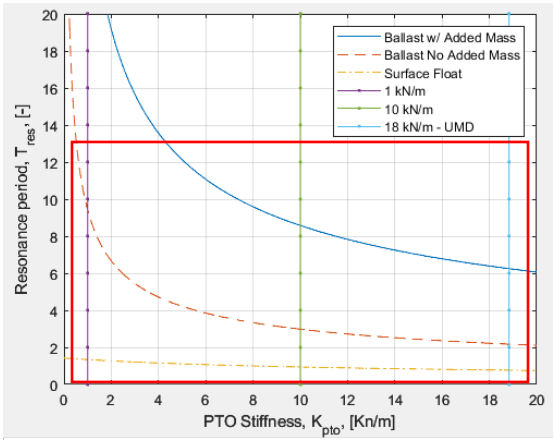

Figure 49: Resonance periods associated with the surface float and ballast with and without added mass.

The initial results from this award caused UMD and the WEC-Sim facility to re-evaluate their assumptions about the model performance and use reduced order modeling tools to better understand the physics of the MADWEC. Unexpected behavior at certain wave frequencies when simulating the base WEC-Sim model could not be explained until the natural frequencies of the ballast and the surface float were estimated. The initial model development utilized a relatively soft PTO stiffness which resulted in a resonance frequency dropping into the wave frequencies of interest when the ballast did not have added mass active. This was causing unexpected drift behavior at approximately a 9 s wave period. At the same time, Version 1 of UMD's PTO model came with an PTO stiffness much higher which then caused the resonance frequency for the ballast with added mass to drop into the wave frequency range of interest. However, in reality the simulations with the bi-directional added mass are jumping between the blue and red dashed lines in Figure 49: Resonance periods associated with the surface float and ballast with and without added mass.Figure49 during each wave cycle which is likely causing the stronger than expected non-sinusoidal responses of the WEC-Sim model.

This realization prompted the WEC-Sim facility to complete a brief frequency domain analysis, ignoring the bi-directional added mass momentarily, to estimate the amplitudes of motion and natural frequencies of the MADWEC system. The frequency domain analysis consisted of developing the impedance matrices that describe the dynamics of the surface float and the PTO Chamber & Ballast, as the two were fixed together in the WEC-Sim model. The following matrix was calculated using the hydrodynamic coefficients from WAMIT, mass properties, and chosen PTO stiffness and damping coefficients.

$$Z = \begin{bmatrix} K_{33} + K_{PTO} - \omega^2\big(m_{33} + \mu_{33}(\omega)\big) + i\omega(\lambda_{PTO} + \lambda_{33}) & -K_{PTO} - \omega^2\mu_{39}(\omega) + i\omega(\lambda_{39} - \lambda_{PTO}) \\ -K_{PTO} - \omega^2\mu_{93}(\omega) + i\omega(\lambda_{93} - \lambda_{PTO}) & K_{99} + K_{PTO} - \omega^2\big(m_{99} + \mu_{99}(\omega)\big) + i\omega(\lambda_{PTO} + \lambda_{99}) \end{bmatrix}$$

If the hydrodynamic cross coupling terms are ignored, which is a reasonable approximation given the spacing between bodies, the impedance matrix can be simplified to the following expression:

$$Z = \begin{bmatrix} K_{33} + K_{PTO} - \omega^2\big(m_{33} + \mu_{33}(\omega)\big) + i\omega(\lambda_{PTO} + \lambda_{33}) & -K_{PTO} - i\omega\lambda_{PTO} \\ -K_{PTO} - i\omega\lambda_{PTO} & K_{99} + K_{PTO} - \omega^2\big(m_{99} + \mu_{99}(\omega)\big) + i\omega(\lambda_{PTO} + \lambda_{99}) \end{bmatrix}$$

With the wave-excitation force values known, the frequency domain response of the two-body system can be calculated by solving a system of equations defined by:

$$Z\begin{bmatrix}\xi_1 \\ \xi_2\end{bmatrix}/A = \begin{bmatrix}X_3 \\ X_9\end{bmatrix}$$

where $\xi_1$is the complex amplitude of motion for the surface float, $\xi_2$is the complex amplitude of motion for the PTO chamber and ballast, X_3 is the complex wave-excitation force per wave amplitude for the surface float, and X_9 is the complex wave-excitation force per wave amplitude for the PTO chamber and ballast. At each wave frequency, the frequency dependent hydrodynamic coefficients can be updated and the equation of motion solved to generate response curves of magnitude and phase as shown in Figure 50850 after selecting a pair of PTO spring and damping coefficients, K_{PTO} and λ_{PTO} respectively. Note this analysis does not account for the bi-directional added mass implementation; however, when compared to the time domain WEC-Sim simulations the wave frequencies with amplified motion were aligned which was the key emphasis behind this reduced order modeling to understand the underlying physics of the two-body WEC system.

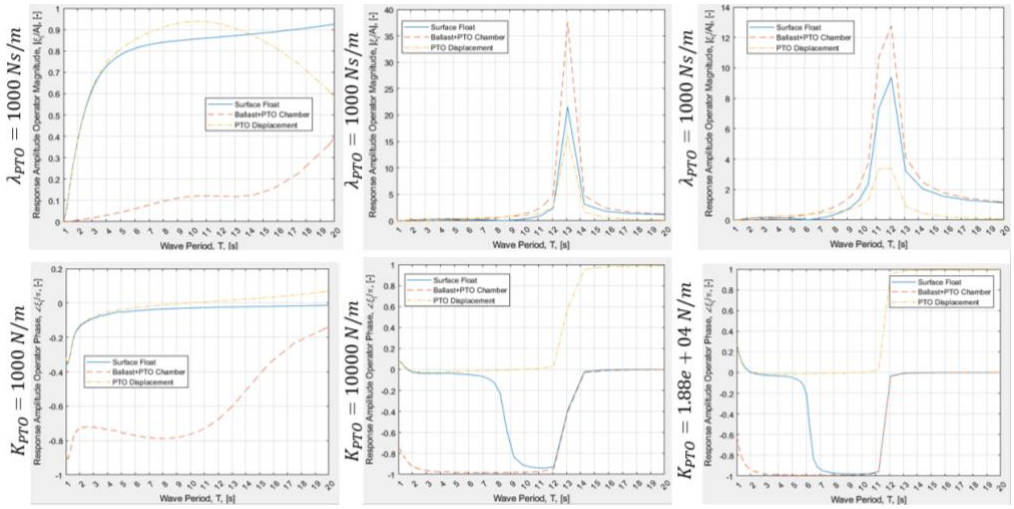

Figure 508: Results from the frequency domain analysis for three pairs of PTO spring and damping coefficients.

After the frequency domain results were presented to UMD, there was a discussion on evaluating how the changing the mass properties and PTO stiffness would impact the MADWEC response. The following configurations were proposed by UMD to be run using the frequency domain analysis:

Buoyancy (kg):

- If you decrease the ballast mass to decrease pre-tension and associated spring stiffness
  - If you do not add mass to the surface float to compensate, there will be excess buoyancy in the surface float and the entire system will move up
- -488 kg
  - Surface float 157 kg, ballast 2251 kg, PTO stiffness 18,833 N/m (assuming 0.25 m of line reel out)
- -400 kg
  - Surface float 245 kg, ballast 2163 kg, PTO stiffness 15,422 N/m (assuming 0.25 m of line reel out)
- -200 kg
  - Surface float 445 kg, ballast 1963 kg, PTO stiffness 7,669.86 N/m (assuming 0.25 m of line reel out)
- -100 kg
  - Surface float 545 kg, ballast 1863 kg, PTO stiffness 3,793 N/m (assuming 0.25 m of line reel out)

The results from the frequency domain analysis are shown in Figure 51951 where the net buoyancy between the surface float and ballast change the system resonance moves to longer wave periods with some rather extreme amplitudes of motion at the higher stiffness values. These results highlighted the impact of the various hydrodynamic and mass properties had on the overall MADWEC performance. Furthermore, the very large amplitudes of motion highlighted that the wave damping provided by linear hydrodynamic theory was insufficient to dampen the ballast motion and follow-on work would also benefit from estimating and incorporating viscous damping forces that will help reduce the large response peaks but is not captured using linear potential flow models.

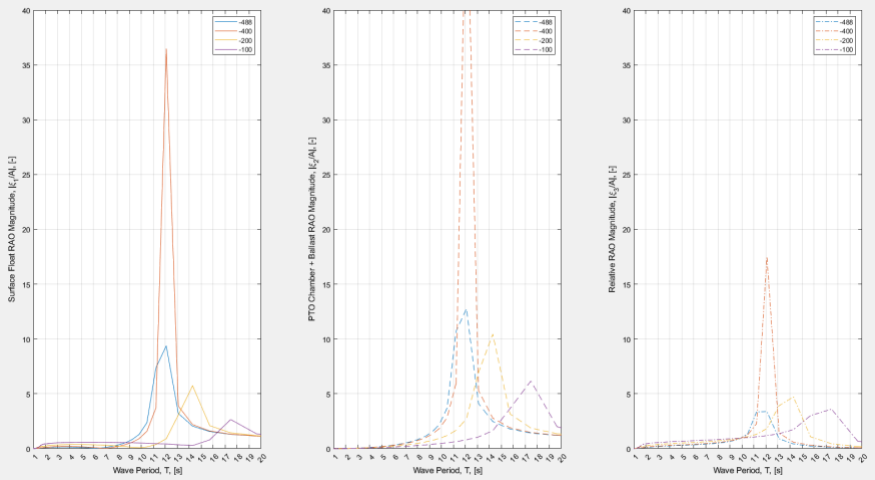

Figure 519: Frequency domain response of the two body WEC assuming different mass and pretension values between the surface float and the ballast system.

Lastly, the frequency domain model was used to artificially increase the ballast added mass by 10x to see if a revised MADWEC device needed to increase the number of buckets to get the desired reaction force. The preliminary results can be found in Figure 521052, which does provide evidence that increasing the number of bucket ballast systems would reduce the total amplitudes of motion to provide a more stationary ballast body.

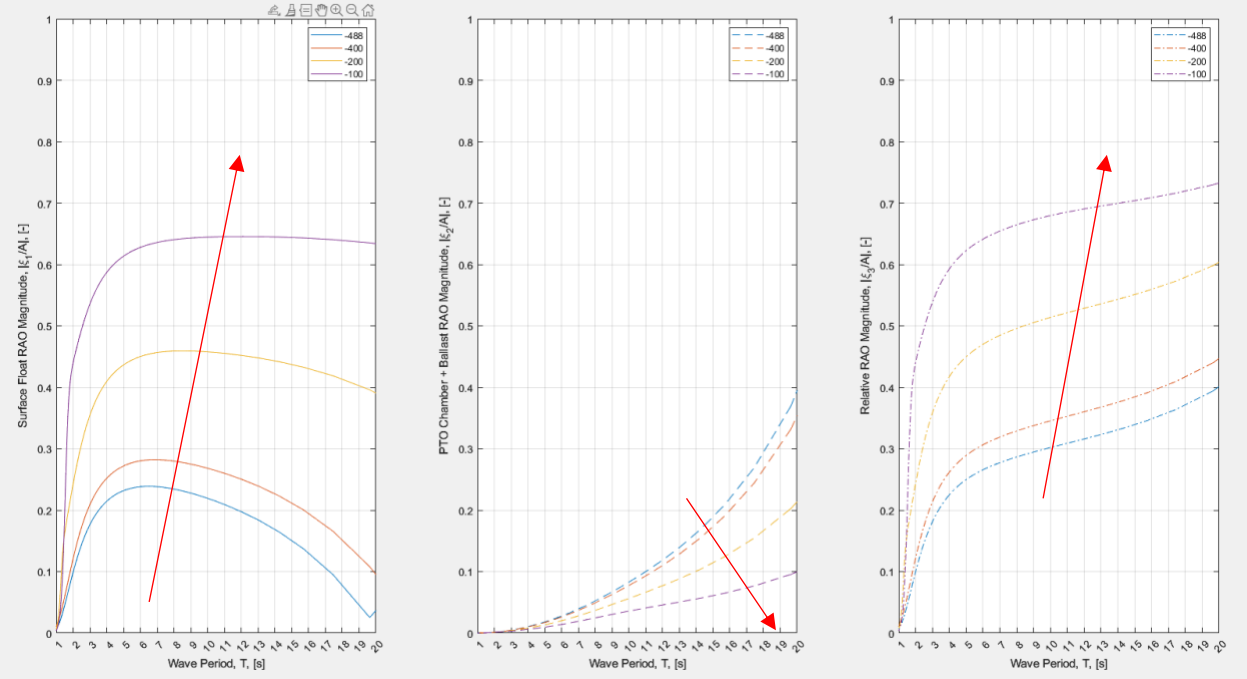

Figure 5210: Frequency domain response of the two body WEC assuming different mass and pretension values between the surface float and the ballast system while also artificially increasing the ballast added mass by a factor of 10.

The WEC-Sim results combined with the frequency domain analysis assisted in providing a better understanding of how the MADWEC system responded to the range of system parameters. The initial

MADWEC design will need to be modified to achieve a more desirable performance and the opportunity to complete this parameter search will hopefully be pursued under a follow-on TEAMER award.

8 CONCLUSIONS AND RECOMMENDATIONS

The University of Massachusetts Dartmouth (UMD) and the WEC-Sim Facility collaborated to develop the first WEC-Sim model of the UMD's Maximal Asymmetric Drag Wave Energy Converter (MADWEC). Prior to developing the WEC-Sim model, this award first explored the hydrodynamic properties of open top cylinders which comprises the nested ballast concept. The first step in the analysis was to explore which diameter and height of the open top cylinders would maximize the heave added mass. After completing a sweep of diameters and heights, for a range of acceptable values provided by UMD, the maximum added mass unsurprisingly corresponded to the largest acceptable values yet the diameter of the cylinder was found to have a nonlinear impact on the added mass. The next step in the added mass analysis was to determine the optimum spacing between two identical open top cylinders to maximize added mass. The original hope was to find a separation distance that would lead to positive interactions between cylinders and increase the added mass above what one would achieve with two cylinders spaced far apart. Unfortunately, the hydrodynamic analysis found that all interaction effects were destructive and the minimum separation distance to recapture the most added mass was equal to the cylinder diameters. This conclusion also held when exploring a three-cylinder configuration providing strong guidance that keeping the open top cylinders further apart will minimize destructive interference. The final step in the hydrodynamic analysis was to analyze the impact of having nested cylinders on added mass. A constant reduction in diameter of each nested cylinder was assumed and the total number of cylinders modeled was limited to the minimum cylinder diameter allowed. Based on the results from the previous subtasks, the results were unsurprising that because of the rapid reduction in diameter the added mass dropped quickly after 6 nested cylinders and the total added mass did increase but the percentage increase quickly converged to less than a percent. Furthermore, it was found that as the nested cylinders became smaller in diameter the material mass, when assuming steel, began to equal or exceed the added mass further reducing the need for more than 6-10 cylinders.

After completion of Task 1, UMD then had the opportunity to select the size and number of open top ballast cylinders that would comprise the ballast system of the full MADWEC system. Once the geometry and mass properties were provided to the WEC-Sim team of the surface float, PTO chamber, and ballast a hydrostatic analysis was completed to confirm the mass and buoyancy properties led to a stable configuration (i.e. the system did not sink or move out of the ocean). After hydrostatic equilibrium was confirmed, each hydrodynamic body was meshed and imported to WAMIT to collect the hydrodynamic coefficients required by WEC-Sim. The hydrodynamic coefficients of all three hydrodynamic bodies were compared and showed that for both the PTO chamber and the ballast system the added mass had minimal frequency variation which is consistent with the depth of submergence where the oscillations could be assumed to oscillate in an infinite fluid where free surface effects are not included which is the cause of the frequency dependence as propagating waves are generated. After establishing a baseline WEC-Sim model, the bi-directional added mass was implemented by creating a custom function that would activate to deactivate the ballast added mass depending on if the ballast system was moving up or down respectively. The result was a slower rise but faster drop in the ballast system during the wave cycle. During this process, UMD was finalizing their custom PTO model which was also integrated into the MADWEC WEC-Sim model which was then simulated in regular and irregular wave conditions to evaluate performance.

During the process of evaluating the WEC-Sim time domain response, unexpected and large oscillations were observed in the model. Initially it was thought that this was caused by errors in the bi-directional added mass implementation; however, upon further investigation the team realized that resonances in the MADWEC system were being excited. If there was no bi-directional added mass, the system would have approximately two resonance periods tied to the oscillation of the surface float and ballast + PTO chamber and the resonance of the lower bodies were being excited resulting in larger periods of oscillations. The team also identified that when the ballast added mass was turned off this would set another resonance frequency of the ballast body which was lower than when the added mass is active. Furthermore, during the wave cycle the added mass is being turned on and off resulting in the introduction of a second harmonic on top of the wave harmonic which can result in triggering the resonance frequency of the ballast without added mass.

After these realizations, the team decided to complete a frequency domain analysis requiring to temporarily step back from bi-directional added mass and PTO force implementations. Such analysis allowed for different system parameters (i.e. mass, added mass, and PTO coefficients) to be iterated over to see how all hydrodynamic bodies responded. The frequency domain analysis results illustrated that the initial MADWEC design likely had 1) too low added mass in the ballast system and 2) the PTO spring stiffness was a major contributor to exciting system resonances. Furthermore, the PTO chamber and ballast system only had wave damping available to dampen motion, but as shown in the hydrodynamic analysis section these values were very small resulting in very large oscillation amplitudes near resonance. A limitation of linear hydrodynamic analysis is that viscosity is ignored, a known limitation of BEM models, and upon reflection the team acknowledged that including some estimate on viscous drag of the ballast system through the water needs to be included to help provide realistic amplitudes of motion.

Both UMD and the WEC-Sim facility believe that although the WEC-Sim model developed as part of this award my not be providing the desired performance the influence in the various model parameters has been highlighted to help UMD determine the second generation MADWEC concept. An RFTS 10 application was submitted to propose follow-on work to this award to address the short comings identified and complete a wider parameter sweep across the various system parameters.

9 REFERENCES

MacDonald, D.G. Tethered Ballast Systems for Point Absorbing Wave Energy Converters and Method of Use Thereof. US Patent Issued 26 October 2021 (US 11,156,200 B2)

Browne, G.E., C. Meninno, W. Michaud, N. White, MacDonald, D.G., M. Raessi. Oscillating Tension Wave Energy Converter, Provisional Patent Application filed 28 April 2020. PCT filed April 2021.

Tarantino, N. J., 2018. Numerical Modeling of a Tethered Ballast for Point Absorber Wave-Energy Converter Technology. M.S. Thesis, University of Massachusetts Dartmouth.

Encarnacion, A., M. Meehan, M. Shonar, K. Andrade, C. Abad, S. Dowty, T. Lattanzi, A. Grizotte, A. Francois, B. Camara, M. Benjamin, D. MacDonald, P. Karlson, M. Raessi. AUV Charging Station Powered by the Maximal Asymmetric Drag Wave Energy Converter (MADWEC). Final Report Submittal to the

2022 Marine Energy Collegiate Competition sponsored by the National Renewable Energy Laboratory, Denver, CO. YouTube Video Link.

10 ACKNOWLEDGEMENTS

The WEC-Sim facility and the University of Massachusetts PIs would like to acknowledge Anthony Encarnacion's contributions to the development of the custom PTO model.

11 APPENDIX

Task 2 Boundary Element Method Modeling

BEM comparison for an open and closed ballast system

The results shown in this section show how the scaling factors between the closed ballast hydrodynamic forces and the open ballast hydrodynamic forces can be chosen. Note the y-axes scales on each plot as they may vastly differ in magnitude.

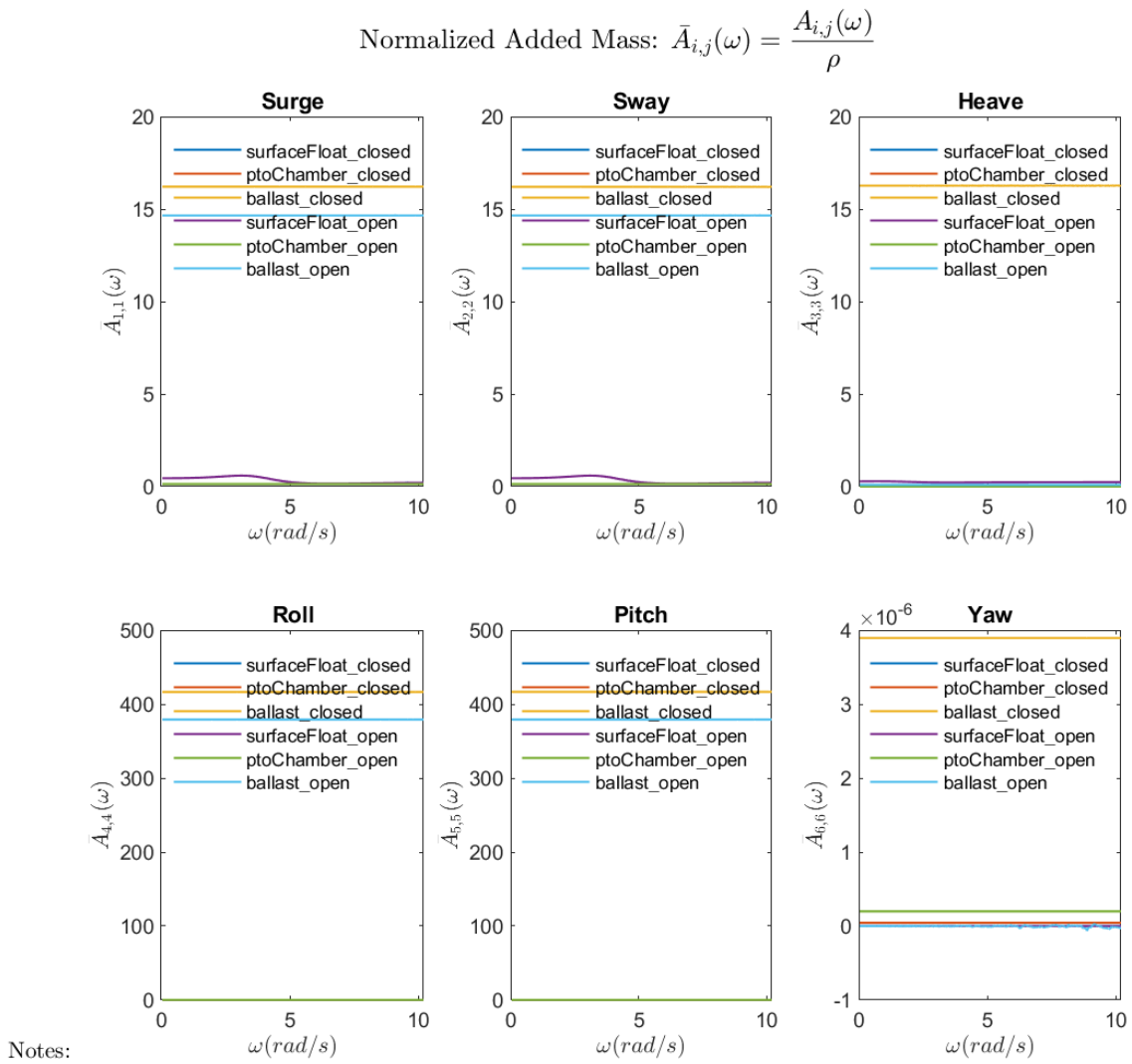

Notes:

- $\bar{A}_{i,j}(\omega)$ should tend towards a constant, A_∞, within the specified ω range.
- Only $\bar{A}_{i,j}(\omega)$ for the surge, heave, and pitch DOFs are plotted here. If another DOF is significant to the system, that

Figure A1. Added mass from the closed and open ballast systems.

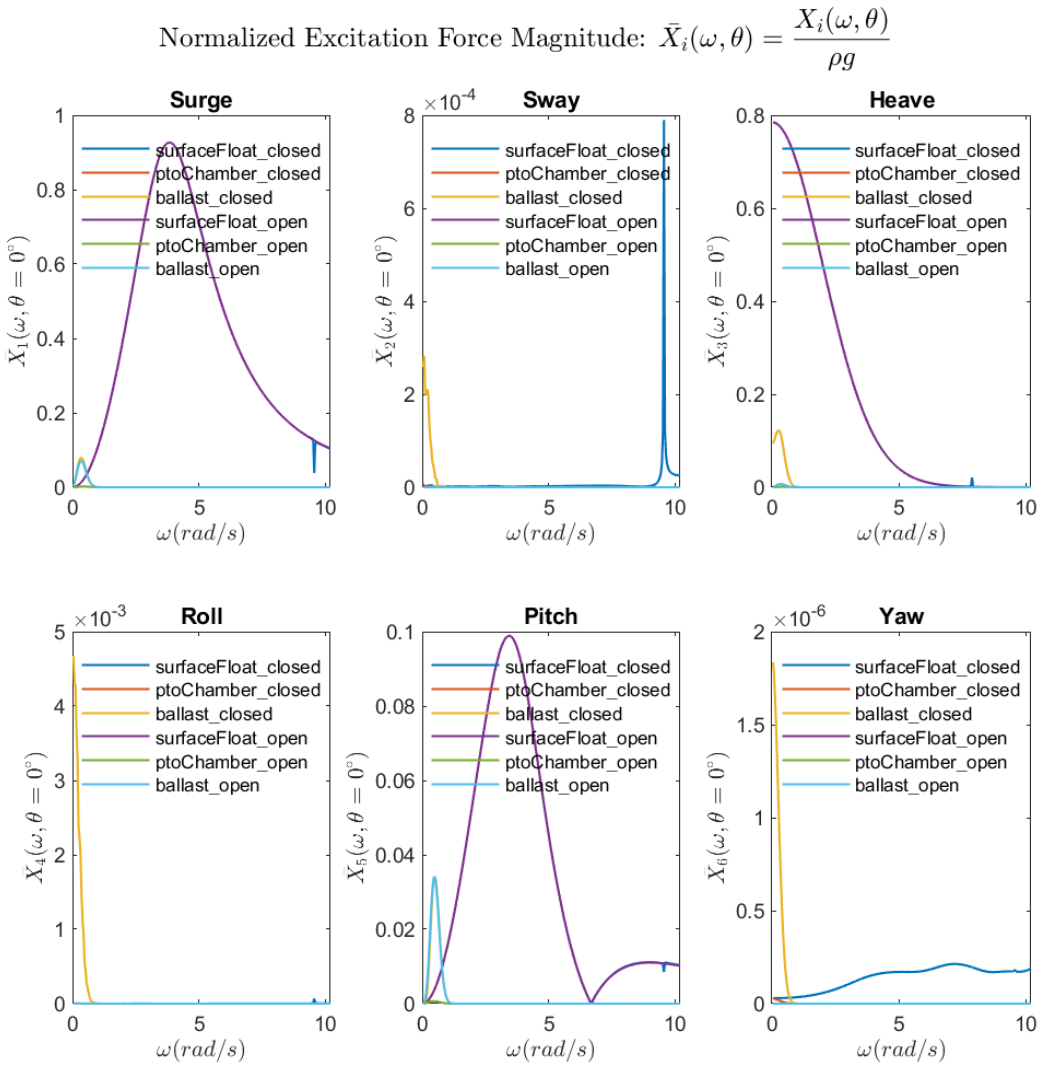

Figure A2. Radiation damping from the closed and open ballast systems.

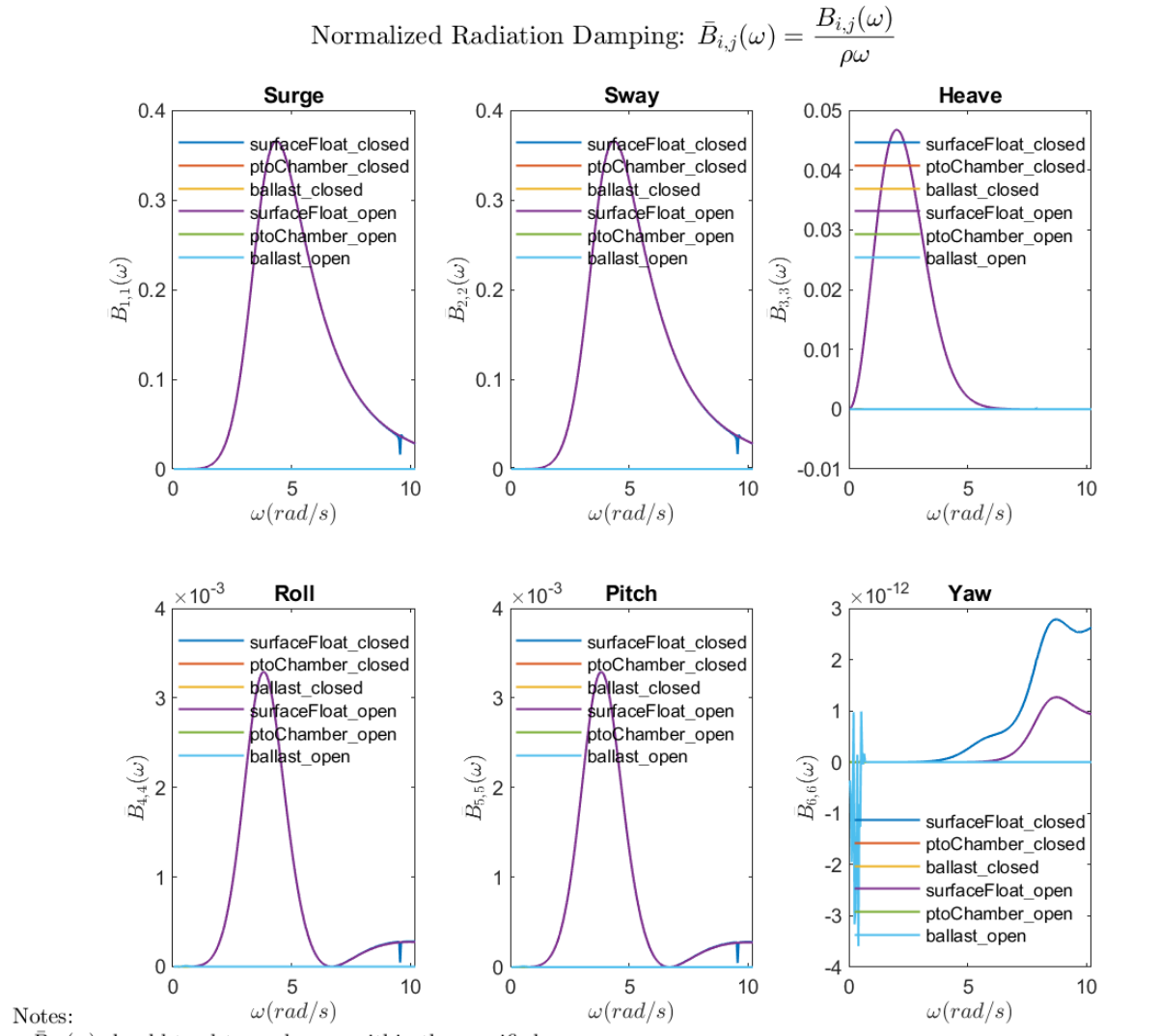

Notes:
- $\bar{B}_{i,j}(\omega)$ should tend towards zero within the specified ω range.
- Only $\bar{B}_{i,j}(\omega)$ for the surge, heave, and pitch DOFs are plotted here. If another DOF is significant to the system that

Figure A3. Excitation force from the closed and open ballast systems.

Bidirectional Added Mass Tests

As described in Section 7.1, the bidirectional added mass is a new feature within WEC-Sim. Several numerical tests were completed to assess the validity of the implementation. The results of those tests are detailed here for reference and to provide confidence in the specialized added mass implementation. The 6 second period and 8 second period are chosen to highlight the affects that the PTO mass-spring-damper system can have on the model results, especially when the PTO natural frequency aligns with the incoming wave frequency.

As shown below, the numerical options (wave type, time step, scaling method) do not significantly affect either the 6s or 8s wave. The wave period and its relation to the PTO stiffness and damping are

especially important however. The bidirectional hydrodynamics act as expected across wave period, except when the wave period corresponds to the dominant natural frequency of a mass-spring-damper PTO. All plots show the ballast heave response relative to its initial position.

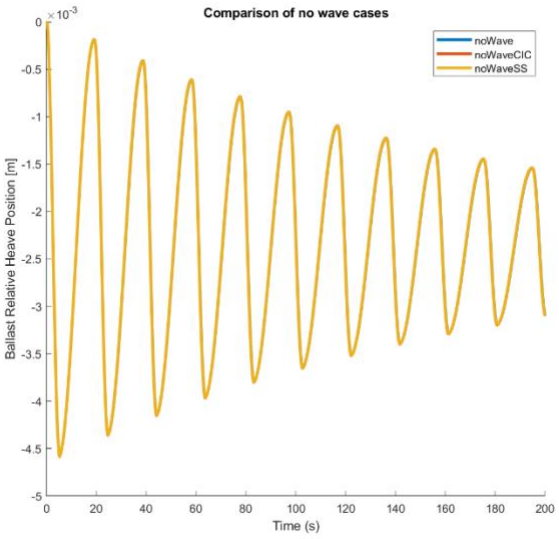

Figure A4. Comparison of various no wave cases (noWave, convolution integral, state space).

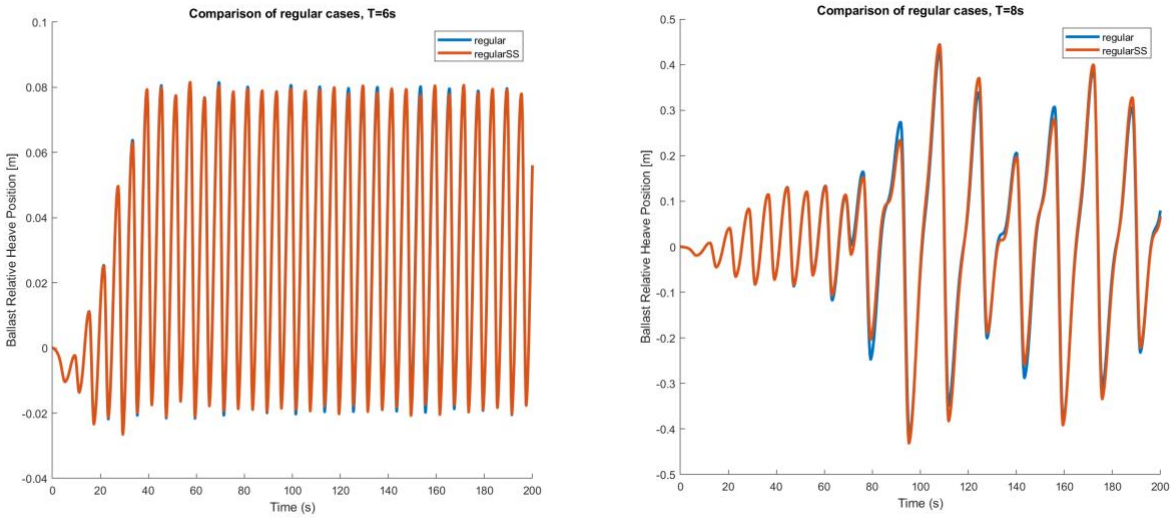

Figure A5. Comparison of various regular waves (regular and state space) with 6 second period (left) and with 8 second period (right).

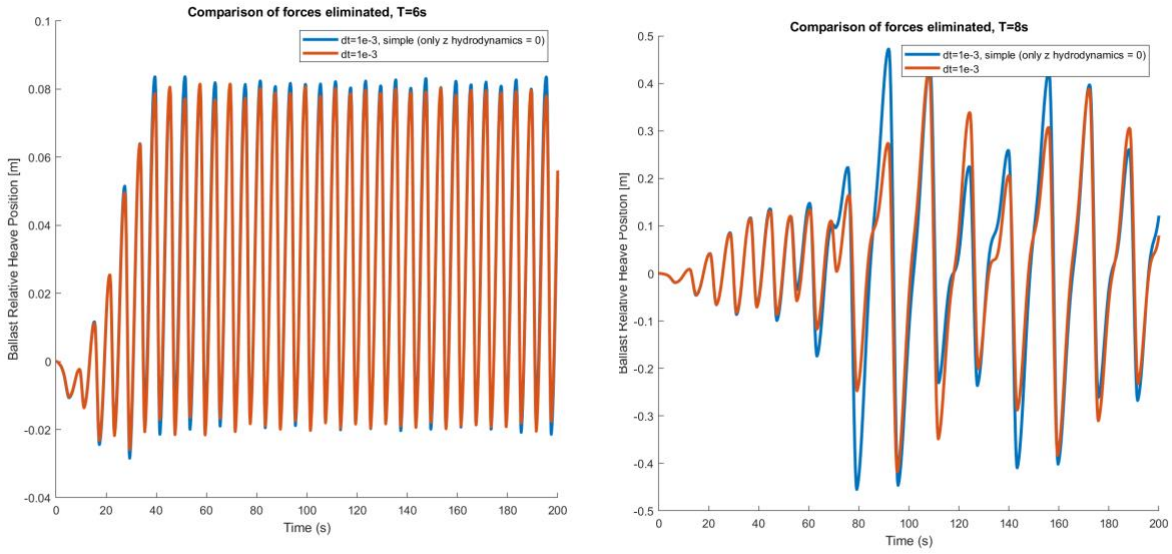

Figure A6. Comparison of hydrodynamic methods: using scaled ratios described in Section 7 (orange) and completely eliminating heave forces for open louvers (blue). 6 second period (left), 8 second period (right).

Figure A7 shows how the model degrades and becomes unstable when the simulation time step is too large. This is expected for a large time step and a custom model. Figure A8 shows the time step comparison without 10^-1 and how the 10^-2 is not quite converged. The model appears fully converged when using a time step on the order of 10^-3.

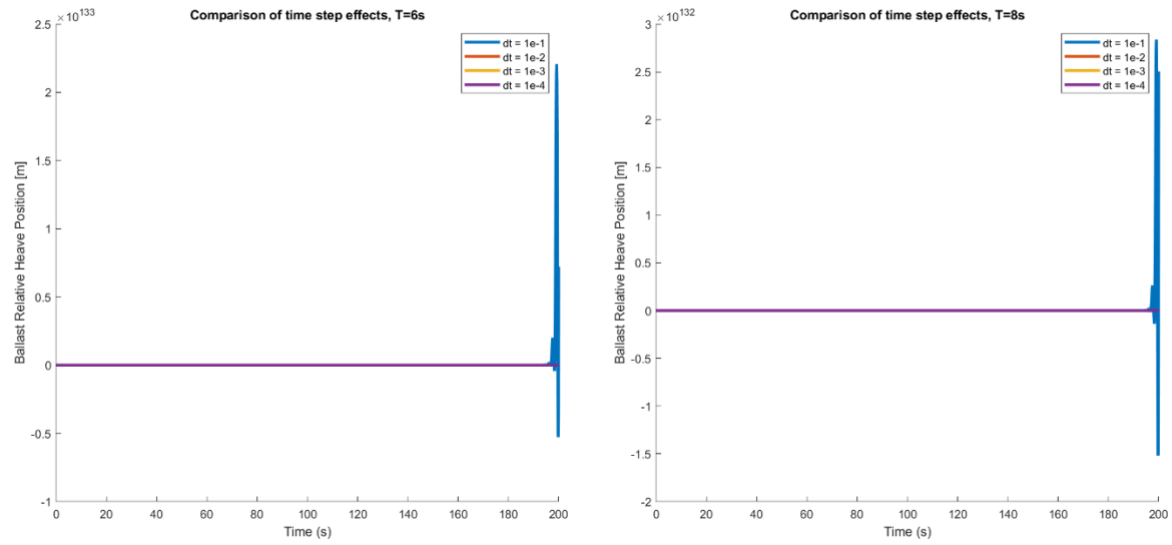

Figure A7. Comparison of time step effects. 6 second period (left) and 8s period (right).

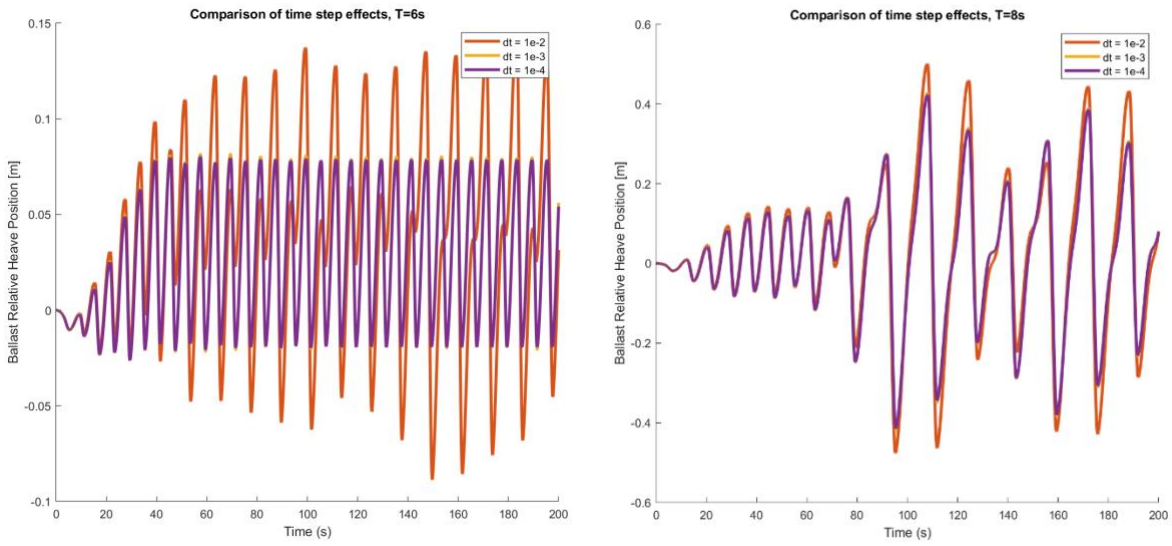

Figure A8. Comparison of time step effects, with dt = 10^-1 removed. 6 second period (left) and 8s period (right).

This visualization of irregular Jonswap waves with a peak period of 6 seconds and 8 seconds, show how the instability seen above is still present for 8 second irregular waves. At the 170 second mark, the model becomes unstable under 8 second waves and greatly increases its motion, just as in the regular wave conditions.

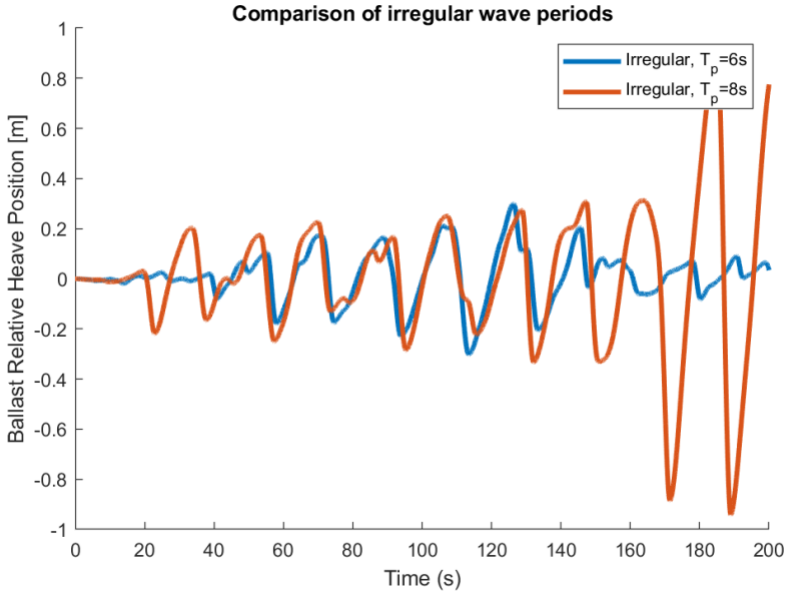

Figure A9. Model performance in irregular waves of 6 second and 8 second peak period.

The follow plots show how the model instability, seen in all the above 8 second wave period plots, is isolated and correlated to the dominant PTO frequency, which in turn is determined by the PTO stiffness and damping. Wave periods of 10 seconds and 8 seconds correspond to the dominant PTO frequency, which makes the model unstable when the hydrodynamic forces are eliminated on the downstroke. The lower periods act as expected, with the ballast period matching the wave period but ascending slowly and descending quickly.

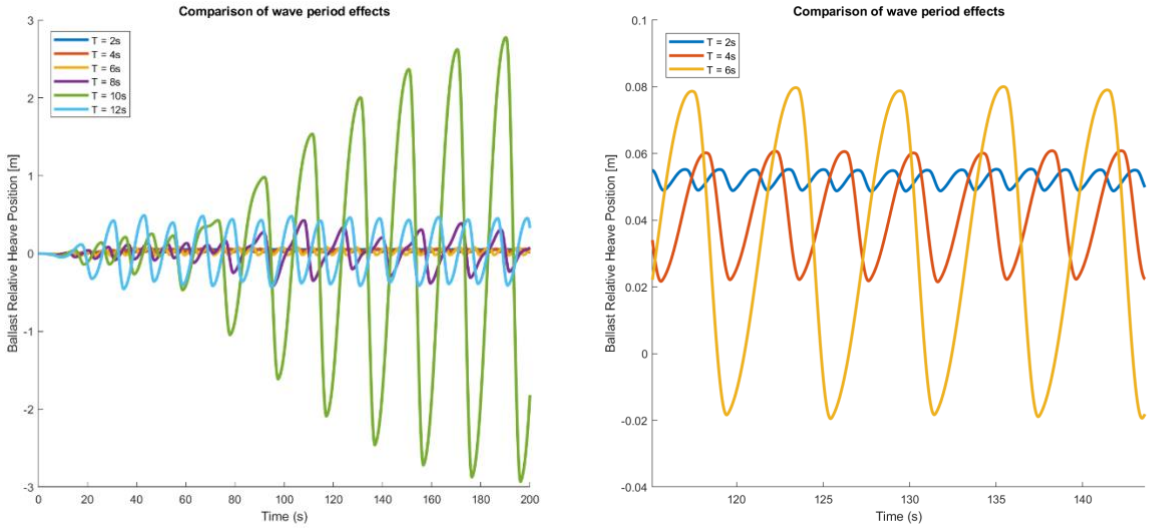

Figure A10. Comparison of wave periods for given PTO parameters (k=1000 N/m, c=100 N/(m/s)). Plots show identical data, but outliers (8s, 10s) are removed on the right.

This final test shows how the ballast heave response for an 8 second wave changes under various PTO parameters. The above tests confirm that the bidirectional added mass implementation is sound and that the additional low-frequency affects seen for 8 second wave periods is driven by the properties of the PTO.